


Penumbra-targeted CircOGDH siRNA-loaded nanoparticles alleviate neuronal apoptosis in focal brain ischaemia

Yanfang Liu,^{1,2,3} Tianyuan Zhang,^{1,2,3} Xing Zou,^{1,2,3} Zhongwen Yuan,^{1,2} Yufeng Li,^{1,2,3} Jiankun Zang,^{1,2,3} Niu He,^{1,2,3} Lizhen He,^{1,2} Anding Xu ,^{1,2,3} Dan Lu^{1,2,3}

To cite: Liu Y, Zhang T, Zou X, et al. Penumbra-targeted CircOGDH siRNA-loaded nanoparticles alleviate neuronal apoptosis in focal brain ischaemia. *Stroke & Vascular Neurology* 2023;**0**. doi:10.1136/svn-2022-002009

► Additional supplemental material is published online only. To view, please visit the journal online (<http://dx.doi.org/10.1136/svn-2022-002009>).

YL, TZ and XZ contributed equally.

Received 18 September 2022
Accepted 2 May 2023



© Author(s) (or their employer(s)) 2023. Re-use permitted under CC BY-NC. No commercial re-use. See rights and permissions. Published by BMJ.

¹Department of Neurology and Stroke Center, Jinan University First Affiliated Hospital, Guangzhou, Guangdong, China

²Department of Clinical Neuroscience Institute, The First Affiliated Hospital of Jinan University, Guangzhou, Guangdong, China

³Key Lab of Guangzhou Basic and Translational Research of Pan-vascular Diseases, The First Affiliated Hospital of Jinan University, Guangzhou, China

Correspondence to

Dr Dan Lu, Guangzhou, China; ludan@jnu.edu.cn

Dr Anding Xu; tlii@jnu.edu.cn

ABSTRACT

Background Nanoparticles (NPs) are a class of substances that can be loaded with therapeutic agents delivered to specific areas. In our earlier research, we identified a neuron-derived circular RNA (circRNA), circular oxoglutarate dehydrogenase (CircOGDH), as a promising therapeutic target for acute ischaemic stroke. This study dedicated to explore a prospective preliminary strategy of CircOGDH-based NP delivered to the ischaemic penumbra region in middle cerebral artery occlusion/reperfusion (MCAO/R) mice.

Methods Immunofluorescence in primary cortex neurons and in vivo fluorescence imaging revealed endocytosis of Poly(lactide-co-glycolide) (PLGA) poly amidoamine(PAMAM)@CircOGDH small interfering RNA (siRNA) NPs. Western blotting analysis and CCK8 assay were performed to evaluate the apoptotic level in ischaemic neurons treated with PLGA–PAMAM@CircOGDH siRNA NPs. Quantitative reverse transcription PCR experiments, mice behaviour test, T2 MRI analysis, Nissl and TdT-mediated dUTP nick end labeling (TUNEL) co-staining were performed to evaluate the apoptosis level of ischaemic penumbra neurons in MCAO/R mice. Biosafety evaluation of NPs in MCAO/R mice was detected by blood routine examination, liver and kidney function examination and HE staining.

Results PLGA–PAMAM@CircOGDH siRNA NPs were successfully assembled. Endocytosis of PLGA–PAMAM@CircOGDH siRNA NPs in ischaemic neurons alleviated neuronal apoptotic level in vitro and in vivo. Furthermore, mice behaviour test showed that the neurological defects of MCAO/R mice were significantly alleviated after the tail injection of PLGA–PAMAM@CircOGDH siRNA NPs, and no toxic effects were observed.

Conclusion In conclusion, our results suggest that PLGA–PAMAM@CircOGDH siRNA NPs can be delivered to the ischaemic penumbra region and alleviate neuron apoptosis in MCAO/R mice and in ischaemic neurons; therefore, our study provides a desirable approach for using circRNA-based NPs for the treatment of ischaemic stroke.

INTRODUCTION

Ischaemic stroke is a leading cause of disability and mortality worldwide and China faces a great challenge.¹ For optimal treatment results after acute ischaemic stroke (AIS), the ischaemic penumbra tissue must be rescued in a stringent time window. Although

WHAT IS ALREADY KNOWN ON THIS TOPIC

⇒ Nanoparticles (NPs) are reported to be effective vehicles to transport therapeutic agents, including drugs, proteins, vaccines, small interfering RNA (siRNA) and DNA, to the brain. In our previous research, we identified a circular RNA (circRNA), circular oxoglutarate dehydrogenase (CircOGDH), which serve as a penumbra biomarker of patients with acute ischaemic stroke, adenovirus-mediated CircOGDH knockdown ameliorated neuronal apoptosis in permanent middle cerebral artery occlusion (MCAO) mice. In this study, we present a promising nanotherapeutic strategy for CircOGDH-targeting agents during ischaemic reperfusion in ischaemic stroke.

WHAT THIS STUDY ADDS

⇒ Our study indicated that NP delivery is a promising strategy for targeting circRNA during ischaemic reperfusion in ischaemic stroke. We demonstrated that poly(lactide-co-glycolide) poly amidoamine (PAMAM)-mediated in vivo delivery of CircOGDH siRNA improved penumbra neuron survival and neurological function in MCAO/middle cerebral artery reperfusion mice.

HOW THIS STUDY MIGHT AFFECT RESEARCH, PRACTICE OR POLICY

⇒ Our study provides a promising nanotherapeutic strategy for targeting circRNAs during ischaemic reperfusion in ischaemic stroke.

the current guidelines for the clinical treatment of AIS recommends recombinant tissue plasminogen activator and endovascular thrombectomy (EVT) to improve functional recovery, the limited therapeutic time window and the serviceable remedy remain a question.² Moreover, during the ischaemic reperfusion process in EVT, complicated pathophysiological responses can lead to neural loss and blood–brain barrier breakdown.³ Thus, initiatives in new neuroprotective drugs delivered to the brain still need to explore.

Data from the past decades have revealed that nanoparticles (NPs) can be effective vehicles to transport therapeutic agents, including drugs, proteins, vaccines, small

interfering RNA (siRNA) and DNA, to the brain.⁴ The rapid development of nanotechnology has yielded various types of NPs, such as polymer NPs, polymer micelles, liposomes and inorganic NPs.⁴ Poly(lactide-co-glycolide) (PLGA) is an FDA-approved polymer that has been widely used as a drug carrier because of its excellent biocompatibility, biosafety and biodegradability.⁴ PAMAM dendrimers are excellent candidate polymers because of their positive charge, which allows them to form highly stable complexes with negatively charged siRNA; thus, they are commonly used as gene delivery systems.⁵ But an emerging consensus is that beyond their gene delivery effects, PAMAM-type dendrimers (<10 nm) also exerts several toxicological actions such as haemolysis and cell death, and removes easily through the blood circulation.^{6,7} Thus PLGA–PAMAM NPs were assembled to minimise the usage amount of PAMAM in the core, and also decreased the strongly positive charge of PAMAM. Research has shown that PLGA biomimetic nanocarriers loaded with human fat extract can increase neurobehavioral recovery in ischaemic stroke,⁸ and PAMAM dendrimer NPs can be taken up by neurons after focal brain ischemia.⁵ Actually, there are series of NPs for RNA therapeutics delivery, NP-based targeting and delivery approaches are becoming promising strategy for effective treatments in ischaemic stroke.⁹

Circular RNAs (circRNAs) are a type of non-coding RNAs that are found in various species and are more stable than linear RNA.¹⁰ They can interact with microRNAs and RNA-binding proteins that affect axon growth, neuronal apoptosis and autophagy—processes that are critical in the pathogenesis of ischaemic stroke.^{11–16} In our previous research, we observed that a circRNA derived from oxoglutarate dehydrogenase (OGDH), CircOGDH, was significantly upregulated in the plasma of AIS patients and penumbra neurons of middle cerebral artery occlusion (MCAO) mice. Furthermore, adenovirus-mediated CircOGDH knockdown ameliorated neuronal apoptosis in MCAO mice and ischaemic neurons. These results indicate that CircOGDH is a potential therapeutic target in patients with AIS.¹¹ Moreover, studies have reported that gold NPs conjugated with CircDNMT1 siRNA are a potential treatment for breast cancer.¹⁷ Poly(β -amino ester) NPs loaded with CircMDK siRNA were reported as a therapeutic strategy to treat hepatocellular carcinoma.¹⁸ These studies indicate that NP delivery is a promising strategy for targeting circRNAs.

In this study, we assembled PLGA–PAMAM@CircOGDH siRNA NPs and demonstrated that PLGA–PAMAM-mediated *in vivo* delivery of CircOGDH siRNA improved penumbra neuron survival and neurological function in middle cerebral artery occlusion/reperfusion (MCAO/R) mice. Our study provides a promising nanotherapeutic strategy for circRNA-targeting agents during ischaemic reperfusion in ischaemic stroke.

MATERIALS AND METHODS

Detailed experimental procedures were provided in the online supplemental file.

RESULTS

Design, assembly and characterisation of PLGA–PAMAM@CircOGDH siRNA NPs

PLGA–PAMAM and PLGA–PAMAM@CircOGDH siRNA NPs were assembled as illustrated in [figure 1A](#). The PAMAM dendrimers displayed a positive charge and formed high-stability complexes with the negatively charged siRNA via electrostatic interaction; therefore, a Zetasizer Nano ZS particle analyzer was used to examine the zeta potential of the PLGA, PAMAM, PLGA–PAMAM and PLGA–PAMAM@CircOGDH siRNA NPs. The zeta potential of the PLGA–PAMAM@CircOGDH siRNA NPs was significantly lower compared with that of PLGA–PAMAM NPs ([figure 1B](#)), indicating that PLGA–PAMAM@CircOGDH siRNA NPs were successfully assembled. The particle size distribution demonstrated a similar range of sizes for PLGA–PAMAM (165 \pm 2.8 nm) and PLGA–PAMAM@CircOGDH siRNA NPs (163 \pm 10.3 nm) ([figure 1C](#)). In addition, the morphology of PLGA–PAMAM and PLGA–PAMAM@CircOGDH siRNA NPs was characterised by transmission Electron Microscope (TEM). The TEM images ([figure 1D](#)) revealed that the two types of NPs had a different morphology, and element mapping showed that C, O, N and P are present (online supplemental figure 1A), indicating that PLGA–PAMAM@CircOGDH siRNA NPs were successfully assembled. Agarose gel electrophoresis was used to analyse the binding capability of NPs when combined with siRNA. As shown in [figure 1E](#), the migration of the PLGA–PAMAM@CircOGDH siRNA NPs was completely inhibited, whereas that of CircOGDH siRNA alone was not. Furthermore, as NP stability is an important parameter for siRNA delivery, first, the size changes were detected in Fetal bovine serum (FBS) solution, which mimics a human physiological environment, and we found PLGA–PAMAM@CircOGDH siRNA NPs maintained at similar size (online supplemental figure 1B,C). Next, NPs were assembled using Cy3-labelled CircOGDH siRNA to form PLGA–PAMAM@Cy3-CircOGDH siRNA NPs. The extension time of PLGA–PAMAM@Cy3-CircOGDH siRNA NPs had no effect on the ultraviolet–visible (UV–Vis) ([figure 1F](#)) or fluorescence ([figure 1G](#)) spectra at different time points.

PLGA–PAMAM@CircOGDH siRNA NPs ameliorates neuronal apoptosis *in vitro*

Subsequently, the cellular uptake of PLGA–PAMAM@CircOGDH siRNA NPs was evaluated. Cy3 labelling revealed that PLGA–PAMAM@cy3-CircOGDH siRNA NPs were taken up by cortical primary neurons *in vitro* ([figure 2A](#)). Previous studies have reported that endocytosis is a key pathway through which NPs enter cells.¹⁹ Thus, the mechanism by which NPs entered neurons was investigated. LysoTracker (cherry) and cy3 (red) labelling

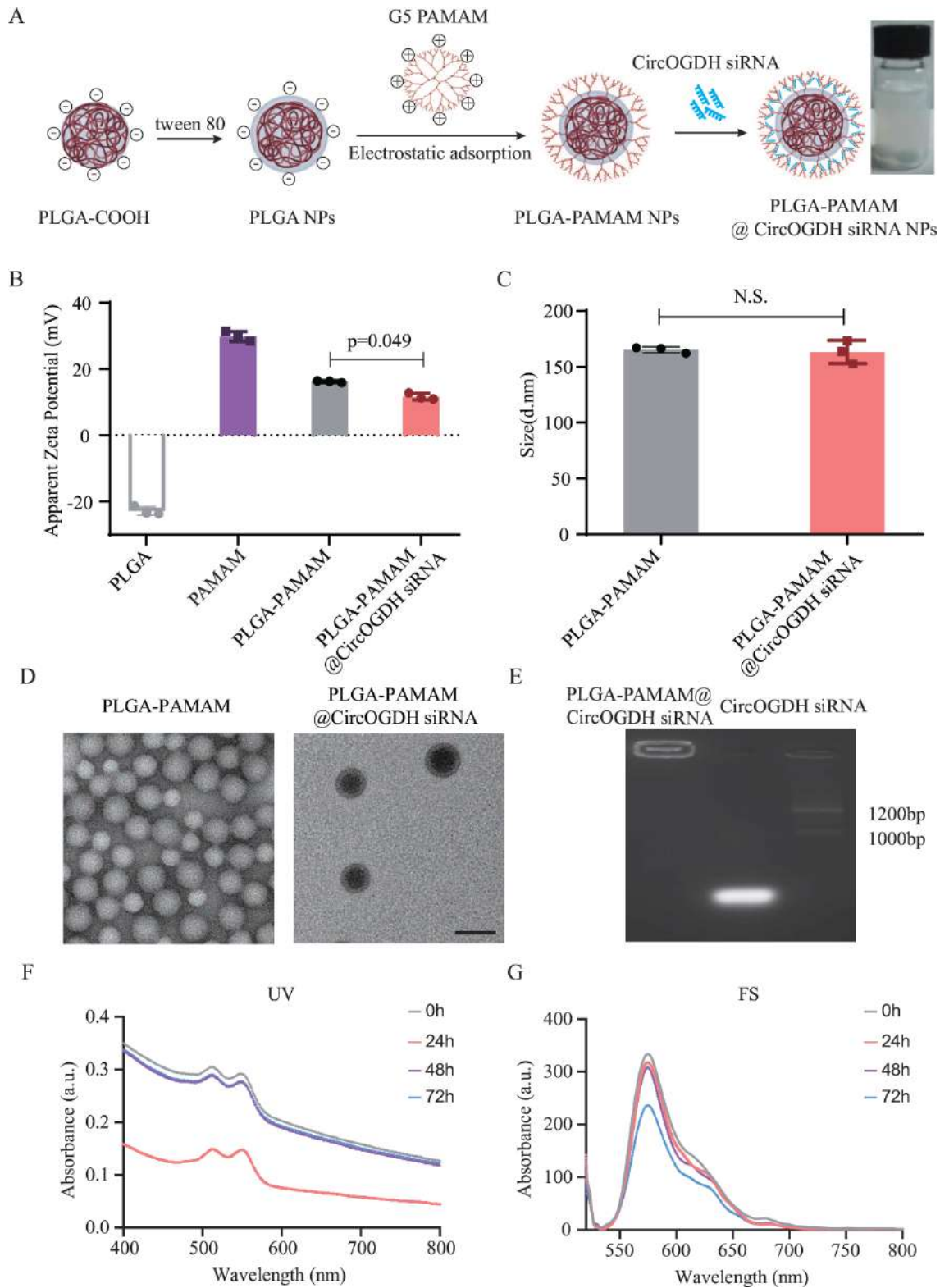


Figure 1 Characterisation of PLGA-PAMAM@CircOGDH siRNA NPs. (A) Schematic illustrations of the assembly of PLGA-PAMAM@CircOGDH siRNA NPs. (B) Zeta potential of PLGA, PAMAM, PLGA-PAMAM and PLGA-PAMAM@CircOGDH siRNA NPs. Data are presented as means \pm SD; n=3 (Mann-Whitney U test). (C) Size distribution of PLGA-PAMAM and PLGA-PAMAM@CircOGDH siRNA NPs. Data are presented as means \pm SD; n=3 (Mann-Whitney U test). (D) TEM images of PLGA-PAMAM and PLGA-PAMAM@CircOGDH siRNA NPs. Scale bar=200 nm. (E) Electrophoretic mobility of siRNA and PLGA-PAMAM@CircOGDH siRNA NPs on agarose gel. Marker: 1000bp DNA ladder. Extension time of PLGA-PAMAM@Cy3-CircOGDH siRNA NPs at 0 hour, 24 hours, 48 hours and 72 hours on the UV-Vis (F) and fluorescence spectra (G). CircOGDH, circular RNAs derived from oxoglutarate dehydrogenase; NPs, nanoparticles; PLGA, poly(lactide-co-glycolide); siRNA, small interfering RNA; UV-Vis, ultraviolet-visible; PAMAM, poly amidoamine); TEM, transmission Electron Microscope .

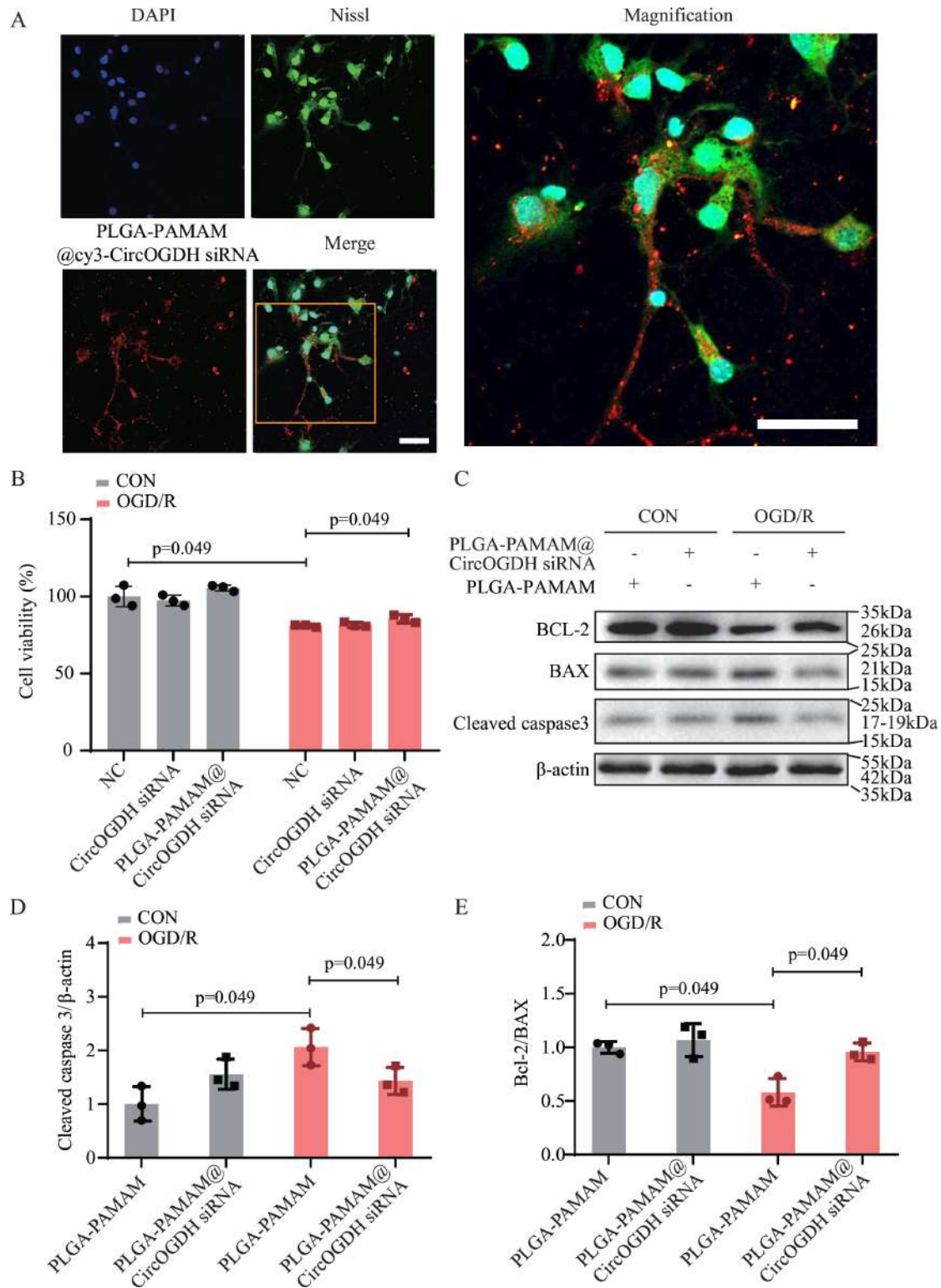


Figure 2 Cellular uptake of PLGA–PAMAM@CircOGDH siRNA NPs. (A) Representative fluorescent microscope images showing the transfection efficiency of PLGA–PAMAM@Cy3-CircOGDH siRNA NPs (red) in primary cortex neurons at 24 hours. Neurons were stained with Nissl (green), and nuclei were stained with DAPI (blue). Scale bar=50 μm. (B) Cell viability was determined in primary cortical neurons treated with NC, CircOGDH siRNA and PLGA–PAMAM@CircOGDH siRNA NPs. Data were presented as mean ± SD; n=3, Mann-Whitney U test. (C–E) Western blot analysis of BAX, BCL2 and cleaved caspase 3 expression levels in CON and ischaemic-reperfusion (OGD/R) neurons treated with PLGA–PAMAM and PLGA–PAMAM@CircOGDH siRNA NPs. Data were presented as mean±SD; n=3, Mann-Whitney U test. CircOGDH, circular RNAs derived from circular oxoglutarate dehydrogenase; CON, control; NC, normal control; NPs, nanoparticles; OGD/R, oxygen and glucose deprivation reperfusion; PLGA, poly(lactide-co-glycolide); siRNA, small interfering RNA; PAMAM, poly amidoamine; DAPI, 4',6-Diamidino-2'-phenylindole.

were chosen to monitor the intracellular localisation of PLGA–PAMAM@CircOGDH siRNA NPs in neurons. The results indicated that PLGA–PAMAM@cy3-CircOGDH siRNA NPs entered neurons via endocytosis beginning at 3 hours after administration and reaching a peak at 9 hours (online supplemental figure 2A). Moreover, we performed flow cytometry analysis in SH-SY5Y cells treated with PLGA–PAMAM@cy3-CircOGDH siRNA NPs and found it can be uptake by SH-SY5Y cells (online supplemental figure 3). These results demonstrate that the assembled PLGA–PAMAM@CircOGDH siRNA NPs can be taken up by cortical primary neurons and SH-SY5Y cells. To further explore the pathophysiological function of PLGA–PAMAM@CircOGDH siRNA NPs in neurons, we established oxygen and glucose deprivation reperfusion model (OGD/R) of neurons. After confirming that PLGA–PAMAM had no effect on neurons (online supplemental figure 2B), we conducted the CCK8 experiment and found that PLGA–PAMAM@CircOGDH siRNA NPs significantly ameliorated neuronal death (figure 2B). And we found that PLGA–PAMAM@CircOGDH siRNA NPs caused an increase of BCL-2/BAX ratio and a decrease of cleaved caspase-3 expression in OGD/R neurons (figure 2C–E). Our previous research indicated that knockdown of CircOGDH ameliorates neuronal apoptosis via targeting miR-5112/COL4A4 mRNA axis, next we detected COL4A4 protein expression level neurons treated with PLGA–PAMAM@CircOGDH siRNA NPs and we found that it caused a decrease of COL4A4 protein expression in OGD/R neurons (online supplemental figure 4), which was consistent with the decrease of COL4A4 mRNA expression in our previous research. Taken together, these results suggest that PLGA–PAMAM@CircOGDH siRNA NPs ameliorate neuronal apoptosis under ischaemic condition *in vitro*.

PLGA–PAMAM@CircOGDH siRNA NPs downregulate CircOGDH expression levels in MCAO/R mice

After confirming that the PLGA–PAMAM@CircOGDH siRNA NPs could be taken up by cortical primary neurons *in vitro*, we focused on their delivery in MCAO mice. Mice underwent MCAO²⁰ for 40 min and reperfusion for 3 days; NPs were administered by tail vein injection every 24 hours during reperfusion (figure 3A). Cerebral blood flow measurement confirmed the success of the MCAO and MCAO/R models (figure 3B). We observed increased uptake of NPs in the penumbra neurons (figure 3C,D), while only a few were localised in microglia and astrocytes (online supplemental figures 5 and 6A), compared with the contralateral tissue of MCAO/R mice after PLGA–PAMAM@Cy3-CircOGDH siRNA NP injection. Furthermore, using Cy5.5-labelled PLGA–PAMAM NPs, we evaluated the biodistribution of PLGA–PAMAM NPs *in vivo* after tail vein injection in MCAO mice by performing fluorescence imaging. The results demonstrated that Cy5.5-labelled PLGA–PAMAM NPs mainly accumulated in the liver and kidneys, but they were also observed in the brain, within an extension time of 0.5 hour, 1.5 hours,

2.5 hours and day 3 (figure 3E, online supplemental figure 6B). Furthermore, quantitative reverse transcription PCR analysis showed that PLGA–PAMAM@CircOGDH siRNA NPs significantly downregulated the CircOGDH expression level in the penumbra tissue of MCAO/R mice (figure 3F). Taken together, these results demonstrate that PLGA–PAMAM@CircOGDH siRNA NPs can be delivered to the brain and significantly downregulate the CircOGDH expression level in the penumbra tissues of MCAO/R mice.

PLGA–PAMAM@CircOGDH siRNA NPs improve neuron survival and neurologic function in MCAO/R mice

Next, we evaluated the neuroprotective effect of PLGA–PAMAM@CircOGDH siRNA NPs in MCAO/R mice. Mice underwent neurological behavioural experiments on day 3 after reperfusion, and their brain tissues were harvested for analysis. After confirmed that PLGA–PAMAM exerted no effect in MCAO/R mice (online supplemental figure 7), we conducted the neurological behavioural experiments and demonstrated that MCAO/R mice injected with PLGA–PAMAM@CircOGDH siRNA NPs exhibited a decreased total time to complete the adhesive removal somatosensory test (figure 4A), a lower ratio of foot faults in the grid-walking test (figure 4B) and a lower ratio of right-biased counts in the cylinder test (figure 4C) compared with the mice in the MCAO/R+PLGA–PAMAM group. Furthermore, we showed that PLGA–PAMAM@CircOGDH siRNA NPs significantly decreased brain infarct size as revealed by T2 MRI (online supplemental figure 8A,B). Nissl staining of brain sections indicated that MCAO/R mice injected with PLGA–PAMAM@CircOGDH siRNA NPs had decreased neuron loss in the penumbra tissue compared with mice in the MCAO/R+PLGA–PAMAM group (figure 4D,E and online supplemental figure 8C). The TUNEL and Nissl co-staining assay of brain sections revealed similar results; MCAO/R mice injected with PLGA–PAMAM@CircOGDH siRNA NPs showed decreased neuron apoptosis in the penumbra tissue compared with mice in the MCAO/R+PLGA–PAMAM group (figure 4F–H). Thus, our results demonstrated that PLGA–PAMAM@CircOGDH siRNA NPs improved neuron survival and neurologic function in MCAO/R mice.

PLGA–PAMAM@CircOGDH siRNA NPs exert no significant toxicity in MCAO/R mice

We next performed haematological and pathological analyses to test the toxicity of these NPs in MCAO/R mice. The haematological analysis showed that the red blood cell (RBC), white blood cell (WBC) and platelet (PLT) levels fluctuated within the normal range in MCAO/R mice injected with PLGA–PAMAM@CircOGDH siRNA NPs or PLGA–PAMAM NPs (online supplemental figure 9). Biochemical analysis of the main organs was conducted by aspartate transaminase, alanine transaminase and creatinine examination, which indicated no obvious injury in MCAO/R mice injected with PLGA–PAMAM@CircOGDH

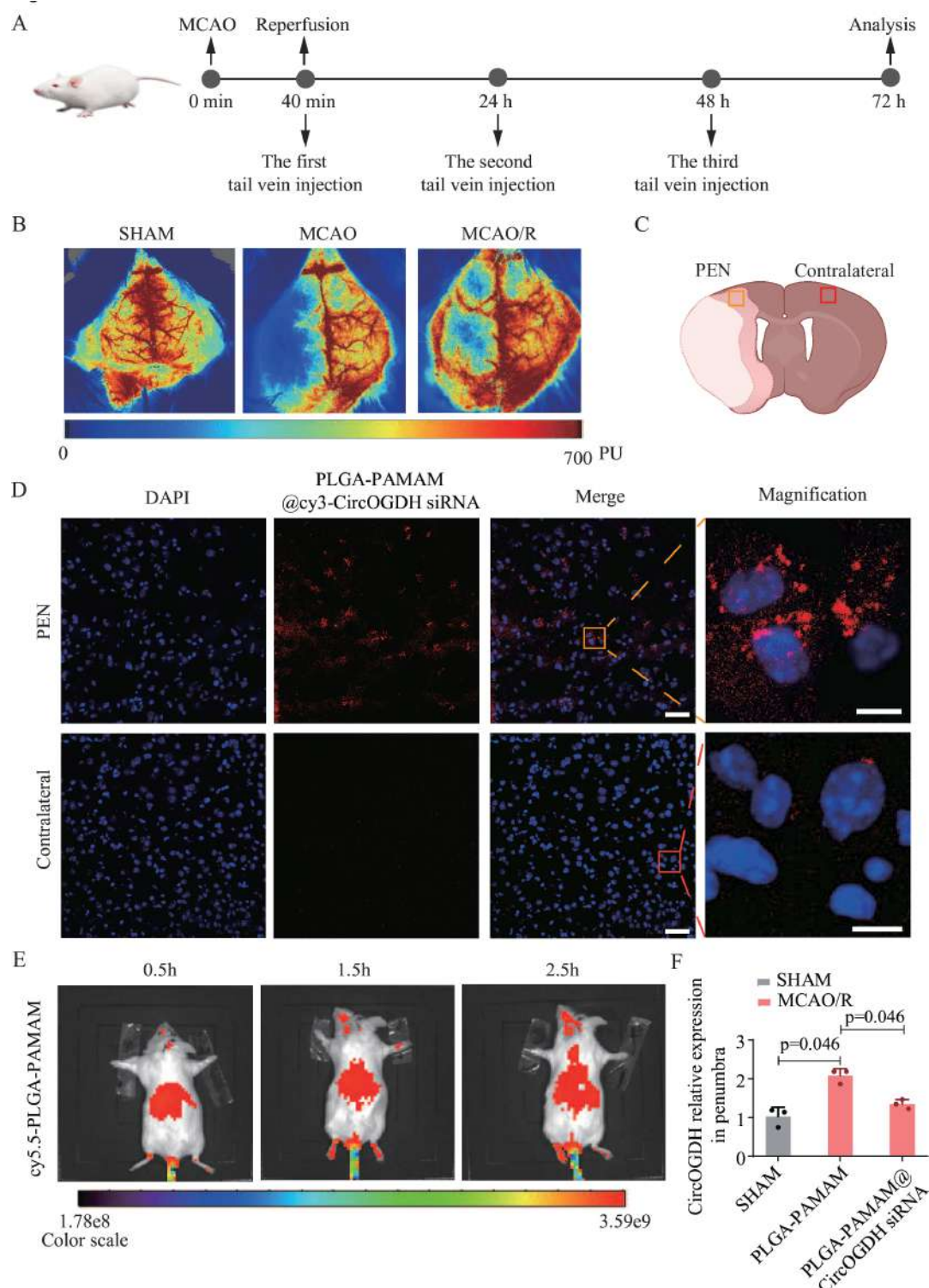


Figure 3 PLGA-PAMAM@CircOGDH siRNA NPs downregulated CircOGDH expression level in MCAO/R mice. (A) Illustration of the in vivo experimental design. (B) Representative images showing the CBF of mice in the SHAM, MCAO and MCAO/R groups. Units of the colour scale: PUs. (C) and (D) Representative fluorescence imaging showing the cellular uptake of PLGA-PAMAM@Cy3-CircOGDH siRNA NPs (red) in the penumbra tissues of MCAO/R mice 3 days after tail injection. Nuclei were stained with DAPI (blue). Scale bar=50 μ m (left), scale bar=10 μ m (right). (E) In vivo fluorescence imaging of Cy5.5-labelled PLGA-PAMAM NPs in MCAO mice at 0.5 hour 1.5 hours and 2.5 hours. Units of the colour scale: PUs. (F) RT-qPCR analysis of the CircOGDH expression level in the penumbra tissues from SHAM and MCAO/R mice after tail injection of PLGA-PAMAM and PLGA-PAMAM@CircOGDH siRNA NPs on day 1. Data are presented as means \pm SD; n=3, Mann-Whitney U test. CBF, Cerebral blood flow; CircOGDH, circular RNAs derived from circular oxoglutarate dehydrogenase; MCAO/R, middle cerebral artery occlusion/reperfusion; NPs, nanoparticles; PLGA, poly(lactide-co-glycolide); PUs, perfusion units; RT-qPCR, quantitative reverse transcription PCR; siRNA, small interfering RNA; PAMAM, poly amidoamine; DAPI, 4',6-Diamidino-2'-phenylindole.

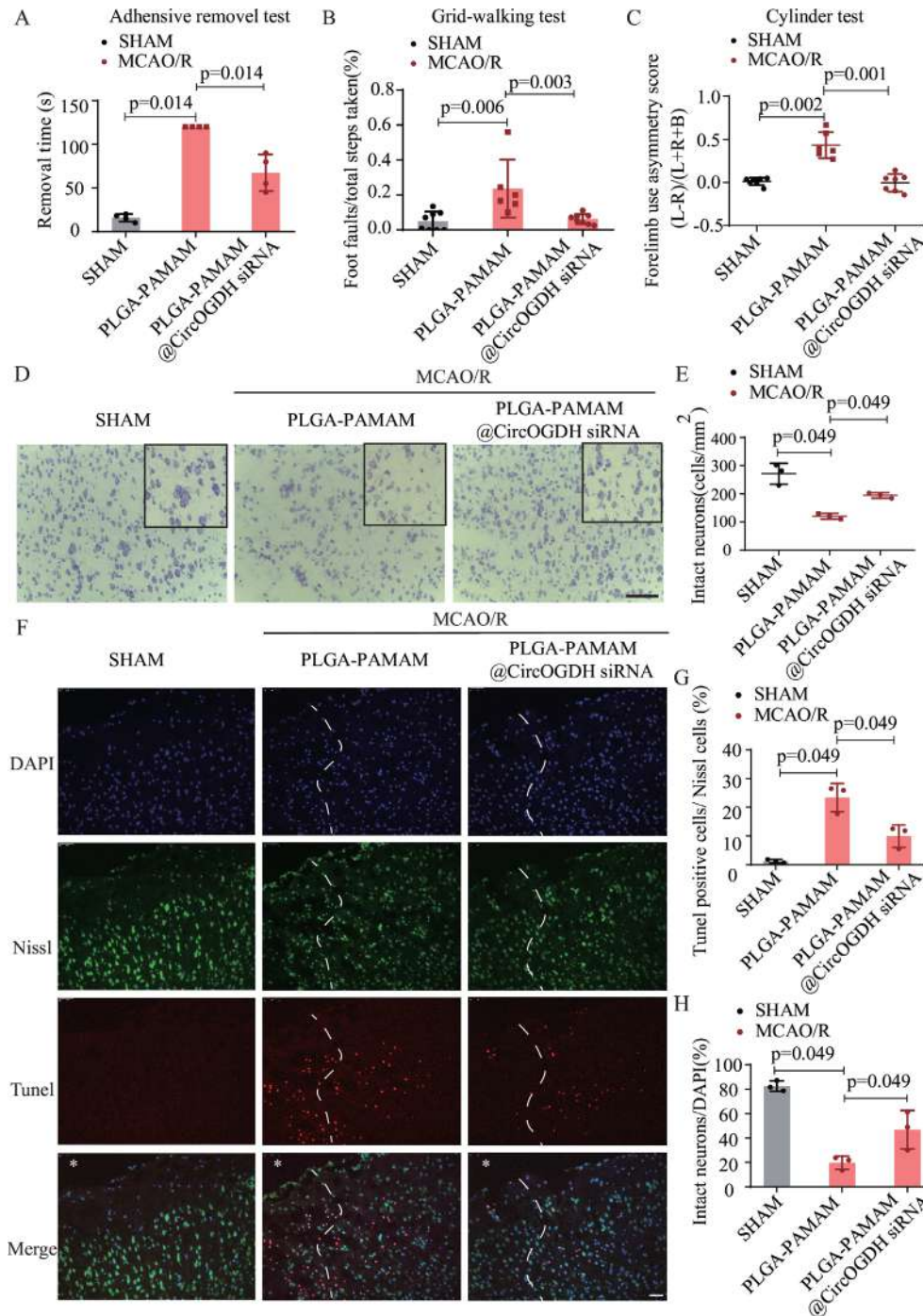


Figure 4 PLGA-PAMAM@CircOGDH siRNA NPs alleviated neuronal apoptosis in MCAO/R mice. PLGA-PAMAM@CircOGDH siRNA NPs improved behavioural recovery in MCAO/R mice 3 days after tail injection, as demonstrated by the adhesive removal test (A), grid-walking test (B) and cylinder test (C). Data are presented as means±SD adhesive removal test: n=4 in each group (Mann-Whitney U test); grid-walking test: n=8 in the SHAM group and the MCAO/R+PLGA-PAMAM@CircOGDH siRNA group, n=6 for MCAO/R+PLGA-PAMAM group (Mann-Whitney U test); cylinder test: n=7 in the SHAM group and the MCAO/R+PLGA-PAMAM@CircOGDH siRNA group (one-way ANOVA followed by Tamhane T2 test). (D) and (E) Nissl staining showing the number of neurons in the SHAM, MCAO/R+PLGA-PAMAM and MCAO/R+PLGA-PAMAM@CircOGDH siRNA groups 3 days after tail injection. Scale bar=100 µm. For the quantification of results in (E), data were presented as mean±SD; n=3, Mann-Whitney U test. (F)–(H) TUNEL and Nissl staining of brain sections showing TUNEL-positive and intact neurons in the brains of mice in the MCAO/R+PLGA-PAMAM and MCAO/R+PLGA-PAMAM@CircOGDH siRNA groups 3 days after tail injection. White dashed lines (left) indicate potential infarct regions; yellow dashed lines (right) indicate potential penumbra regions. Scale bar=50 µm. Data were presented as mean±SD; n=3, Mann-Whitney U test. CircOGDH, circular RNAs derived from circular oxoglutarate dehydrogenase; MCAO/R, middle cerebral artery occlusion/reperfusion; NPs, nanoparticles; PLGA, poly(lactide-co-glycolide); siRNA, small interfering RNA; PAMAM, poly amidoamine; ANOVA, analysis of Variance; TUNEL, TdT-mediated dUTP nick end labeling.



siRNA NPs or PLGA–PAMAM NPs (figure 5A–C). Finally, H&E staining revealed that the main organs (the heart, liver, spleen, lungs and kidneys) displayed no observable pathological injuries on day 3 after treatment with PLGA–PAMAM@CircOGDH siRNA NPs or PLGA–PAMAM NPs in MCAO/R mice (figure 5D). Thus, our results indicated that PLGA–PAMAM@CircOGDH siRNA NPs improved penumbra neuron survival and exerted no significant toxicity in MCAO/R mice.

DISCUSSION

The pathological process of ischaemic stroke is complicated and involves inflammation, oxidative stress and excitotoxicity, which lead to neuronal death.²¹ The management of ischaemic stroke largely depends on intervention within a narrow time window, and rescuing the maximum number of ischaemic penumbra neurons is crucial for optimal AIS treatment.²² Mechanical thrombectomy is a well-established treatment used in patients with AIS for proximal large vessel occlusion within a stringent time window.^{23–25} Though the brain blood flow is restored, secondary damage will occur during the ischaemic reperfusion process in ischaemic region after mechanical thrombectomy.⁹ Our previous studies identified and screened a neuron-derived CircOGDH, which was identified as a potential penumbra therapeutic target in AIS. Furthermore, we found that the binding of CircOGDH to microRNA-5112 regulated the downstream COL4A4 expression level, thus to alleviate neuronal apoptotic level under ischaemic conditions in a permanent 3-hour MCAO mouse model without ischaemic reperfusion.¹¹ As numerous neuroprotective agents have failed to show benefit in a Phase III clinical trial of AIS, effective and new treatment strategies that combine reperfusion raised attention.²⁶ In the present study, we assembled PLGA–PAMAM NPs loaded with CircOGDH siRNA and demonstrated that they exerted a potential protective effect in OGD/R primary cortical neurons and MCAO/R mice using a series of experiments.

Neuronal apoptosis is widely recognised as crucial factors during the pathological process of ischaemic stroke. circRNAs are a type of noncoding RNA expressed in tissue-specific, cell-specific and developmental stage-specific patterns, they are abundant in the brain and are more stable than linear RNA.¹⁰ Increasing evidence identified that circRNAs have been implicated in the pathological process of ischaemic stroke,^{27–29} and circRNA-based therapeutics emerge as a potential therapy for various therapeutic areas, such as prophylactic vaccines.³⁰ Our previous studies identified a neuron-derived CircOGDH, which could aggravating neuronal apoptosis and was identified as a potential penumbra biomarker in AIS.¹¹ However, still many challenges remain regarding targeted delivery of circRNAs.³¹ siRNA is one of the meaningful gene silencing tool that has been widely used to control target gene expression in vivo and in vitro. Still many challenges remain regarding siRNA delivery because of

the molecule's rapid enzymatic degradation.^{32 33} Previous studies have reported that NPs loaded with siRNA improve therapeutic efficacy in ischaemic stroke when administered intravenously.^{33 34} In line with these findings, our results indicate that PLGA–PAMAM@CircOGDH siRNA NPs can protect CircOGDH siRNA from enzymatic degradation for 72 hours (according to UV–Vis and fluorescence spectra analysis). PLGA–PAMAM@CircOGDH siRNA NPs can be taken up by ischaemic neurons in vitro and penumbra neurons in MCAO/R mice. We found PLGA–PAMAM@CircOGDH siRNA NPs preferably accumulated in the penumbra area of MCAO/R mice, thus significantly downregulated CircOGDH expression levels in penumbra tissues of MCAO/R mice. Additionally, we demonstrated that PLGA–PAMAM@CircOGDH siRNA NPs alleviated neuronal apoptotic level in ischaemic neurons, and tail injection of PLGA–PAMAM@CircOGDH siRNA NPs significantly decreased brain infarct size and alleviated neurologic function injury and apoptotic level of ischaemic penumbra neurons in MCAO/R mice.

Polymers, lipids, inorganic materials and exosomes can be used in nanostructured gene delivery systems.³⁵ PLGA is an FDA-approved polymer commonly employed in gene and drug delivery systems for clinical use.³⁶ Despite its excellent biocompatibility and biodegradability, PLGA is difficult to load with nucleic acids because it is negatively charged.⁴ Thus, our study assembled PLGA–PAMAM NPs. PAMAM dendrimers are widely used as a nonviral gene carrier because they exhibit positively charged amine groups on their surface and can be internalised into cells by endocytosis; however, the cytotoxic activity of PAMAM dendrimers requires careful attention,^{6 37} which was a limitation of our study. To address this limitation, haematological and pathological analyses were conducted. The results revealed that the biomarkers evaluated in these analyses remained within a normal range in MCAO/R mice injected with PLGA–PAMAM@CircOGDH siRNA NPs or PLGA–PAMAM NPs. Studies have reported that biomimetic NPs exert high blood compatibility and long circulation times^{8 35 38}; and many different nanoplatforms have been used as nanotherapies to provide neuroprotection in brain injury.³⁹ Therefore, after confirming the protective effect of PLGA–PAMAM@CircOGDH siRNA NPs in MCAO/R mice, our future work will be dedicated to optimise our NPs to minimise the toxicity and improve the delivery efficiency targeting the neurons in the brain.

CONCLUSION

In summary, our data showed that we successfully assembled the PLGA–PAMAM@CircOGDH siRNA NPs and found that they could exert protective effects and preserve the integrity of CircOGDH siRNA by preventing potential degradation. We revealed that PLGA–PAMAM@CircOGDH siRNA NPs alleviated neuronal apoptotic level in ischaemic neurons, and tail injection of PLGA–PAMAM@CircOGDH siRNA NPs significantly decreased brain infarct size and alleviated neurologic function injury

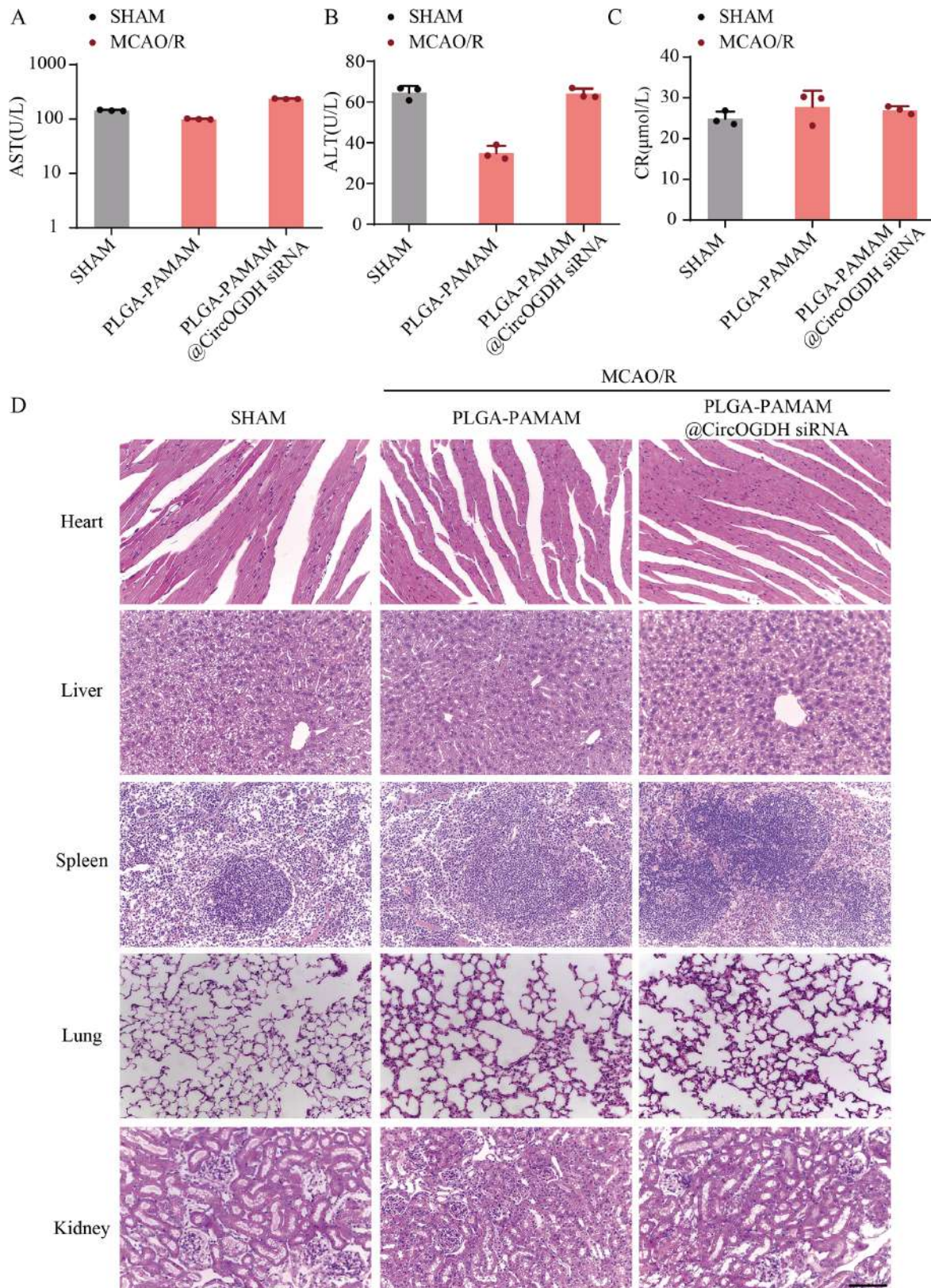


Figure 5 PLGA-PAMAM@CircOGDH siRNA NPs exert no significant toxicity in MCAO/R mice. Haematological analysis of AST (A), ALT (B) and CR (C) were evaluated in the SHAM, MCAO+PLGA-PAMAM and MCAO+PLGA-PAMAM@CircOGDH siRNA groups 3 days after tail injection. Data were presented as mean \pm SD; n=3, Mann-Whitney U test. (D) H&E staining of the heart, liver, spleen, lungs and kidneys in SHAM, MCAO+PLGA-PAMAM and MCAO+PLGA-PAMAM@CircOGDH siRNA mice 3 days after tail injection. Scale bar=100 μm . ALT, alanine transaminase; AST, aspartate transaminase; CircOGDH, circular RNAs derived from circular oxoglutarate dehydrogenase; CR, creatinine; MCAO/R, middle cerebral artery occlusion/reperfusion; NPs, nanoparticles; PLGA, poly(lactide-co-glycolide); siRNA, small interfering RNA; PAMAM, poly amidoamine.

and apoptotic level of ischaemic penumbra neurons in MCAO/R mice. Thus, our study provides a nanotherapeutic strategy for targeting CircOGDH in ischaemic stroke, which may promote the potential clinical transformation of multifunctional nanodrugs targeting circRNA (online supplemental file 2).

Acknowledgements We acknowledge the Guangdong-Hongkong-Macau Institute of CNS Regeneration, Central Laboratory of Basic Medical College and Department of Chemistry of Jinan University for providing the required equipment used in this study. The authors would like to thank TopEdit (www.topeditsci.com) for its linguistic assistance during the preparation of this manuscript.

Contributors YLiu performed experiments, prepared figures, analysed data, wrote, edited and proofread the manuscript. TZ performed experiments and the animal data analysis, prepared figures, wrote, edited and proofread the manuscript. XZ performed experiments and the cell data analysis and prepared figures, wrote, edited and proofread the manuscript. ZY and NH help performed experiments on nanoparticles. YLi and JZ assisted the animal experiments. LH edited and proofread the manuscript. DL and AX conceptualised and directed the overall project. DL and AX are responsible for the overall content as guarantors. The guarantor accepts full responsibility for the finished work and the conduct of the study, had access to the data, and controlled the decision to publish.

Funding This work was supported by grants from the National Natural Science Foundation of China (81801150, 81971121, 82271304, 82171316 and 81671167), the Science and Technology Planning Project of Guangdong Province, China (2017A020215049 and 2019A050513005), Natural Science Foundation of Guangdong Province (2018A0303130182, 2020A1515010279 and 2022A1515012311), the Fundamental Research Funds for the Central Universities (21621102), Science and Technology Projects in Guangzhou, China (2014Y2-00505, 202002020003, 202201010127 and 202201020042) and Clinical Frontier Technology Program of the First Affiliated Hospital of Jinan University, China (JNU1AF-CFTP-2022-a01203).

Competing interests None declared.

Patient consent for publication Not applicable.

Ethics approval Not applicable.

Provenance and peer review Not commissioned; externally peer reviewed.

Data availability statement All data relevant to the study are included in the article or uploaded as supplemental information.

Supplemental material This content has been supplied by the author(s). It has not been vetted by BMJ Publishing Group Limited (BMJ) and may not have been peer-reviewed. Any opinions or recommendations discussed are solely those of the author(s) and are not endorsed by BMJ. BMJ disclaims all liability and responsibility arising from any reliance placed on the content. Where the content includes any translated material, BMJ does not warrant the accuracy and reliability of the translations (including but not limited to local regulations, clinical guidelines, terminology, drug names and drug dosages), and is not responsible for any error and/or omissions arising from translation and adaptation or otherwise.

Open access This is an open access article distributed in accordance with the Creative Commons Attribution Non Commercial (CC BY-NC 4.0) license, which permits others to distribute, remix, adapt, build upon this work non-commercially, and license their derivative works on different terms, provided the original work is properly cited, appropriate credit is given, any changes made indicated, and the use is non-commercial. See: <http://creativecommons.org/licenses/by-nc/4.0/>.

ORCID iD

Anding Xu <http://orcid.org/0000-0003-3154-0985>

REFERENCES

- Wang Y-J, Li Z-X, Gu H-Q, *et al.* China Stroke Statistics: an update on the 2019 report from the National Center for Healthcare Quality Management in Neurological Diseases, China National Clinical Research Center for Neurological Diseases, the Chinese Stroke Association, National Center for Chronic and Non-communicable Disease Control and Prevention, Chinese Center for Disease Control and Prevention and Institute for Global Neuroscience and Stroke Collaborations. *Stroke Vasc Neurol* 2022;7:415–50.
- Jadhav AP, Desai SM, Jovin TG. Indications for mechanical Thrombectomy for acute ischemic stroke: Current guidelines and beyond. *Neurology* 2021;97:S126–36.
- Han L, Jiang C. Evolution of blood-brain barrier in brain diseases and related systemic nanoscale brain-targeting drug delivery strategies. *Acta Pharm Sin B* 2021;11:2306–25.
- Li MX, Weng JW, Ho ES, *et al.* Brain delivering RNA-based therapeutic strategies by targeting Mtor pathway for axon regeneration after central nervous system injury. *Neural Regen Res* 2022;17:2157–65.
- Santos SD, Xavier M, Leite DM, *et al.* Pamam Dendrimers: blood-brain barrier transport and neuronal uptake after focal brain ischemia. *J Control Release* 2018;291:65–79.
- Fox LJ, Richardson RM, Briscoe WH. PAMAM Dendrimer - cell membrane interactions. *Adv Colloid Interface Sci* 2018;257:1–18.
- Zhang N, Feng N, Xin X, *et al.* Nano-drug delivery system with enhanced tumour penetration and layered anti-tumour efficacy. *Nanomedicine* 2022;45:102592.
- Wang C, Yang X, Jiang Y, *et al.* Targeted delivery of fat extract by platelet membrane-cloaked nanocarriers for the treatment of ischemic stroke. *J Nanobiotechnology* 2022;20:249.
- Kaviarasi S, Yuba E, Harada A, *et al.* Emerging paradigms in nanotechnology for imaging and treatment of cerebral ischemia. *J Control Release* 2019;300:22.
- Rybak-Wolf A, Stottmeister C, Głażar P, *et al.* Circular RNAs in the mammalian brain are highly abundant, conserved, and dynamically expressed. *Mol Cell* 2015;58:870–85.
- Liu Y, Li Y, Zang J, *et al.* CircOGDH is a penumbra biomarker and therapeutic target in acute ischemic stroke. *Circ Res* 2022;130:907–24.
- Yang Z, Huang C, Wen X, *et al.* Circular RNA Circ-Foxo3 attenuates blood-brain barrier damage by inducing autophagy during ischemia/reperfusion. *Mol Ther* 2022;30:1275–87.
- Wu F, Han B, Wu S, *et al.* Circular RNA TLK1 aggravates neuronal injury and neurological deficits after ischemic stroke via miR-335-3p/TIPARP. *J Neurosci* 2019;39:7369–93.
- Han B, Zhang Y, Zhang Y, *et al.* Novel insight into circular RNA HECTD1 in astrocyte activation via autophagy by targeting Mir142-TIPARP: implications for cerebral ischemic stroke. *Autophagy* 2018;14:1164–84.
- Bai Y, Zhang Y, Han B, *et al.* Circular RNA DLGAP4 ameliorates ischemic stroke outcomes by targeting miR-143 to regulate endothelial-mesenchymal transition associated with blood-brain barrier integrity. *J Neurosci* 2018;38:32–50.
- Li B, Xi W, Bai Y, *et al.* FTO-dependent M(6)A modification of Plpp3 in circSCMH1-regulated vascular repair and functional recovery following stroke. *Nat Commun* 2023;14:489.
- He AT, Liu J, Li F, *et al.* Targeting circular RNAs as a therapeutic approach: current strategies and challenges. *Signal Transduct Target Ther* 2021;6:185.
- Du A, Li S, Zhou Y, *et al.* M6A-mediated upregulation of circMDK promotes tumorigenesis and acts as a nanotherapeutic target in hepatocellular carcinoma. *Mol Cancer* 2022;21:109.
- Rao S, Lin Y, Lin R, *et al.* Traditional Chinese medicine active ingredients-based selenium nanoparticles regulate antioxidant selenoproteins for spinal cord injury treatment. *J Nanobiotechnology* 2022:278.
- Lu D, Liu Y, Mai H, *et al.* Rosuvastatin reduces neuroinflammation in the hemorrhagic transformation after RT-PA treatment in a mouse model of experimental stroke. *Front Cell Neurosci* 2018;12:225.
- Frank D, Zlotnik A, Boyko M, *et al.* The development of novel drug treatments for stroke patients: a review. *Int J Mol Sci* 2022;23:5796.
- Baron JC. Protecting the ischaemic penumbra as an adjunct to thrombectomy for acute stroke. *Nat Rev Neurol* 2018;14:325.
- Nogueira RG, Jadhav AP, Haussen DC, *et al.* Thrombectomy 6 to 24 hours after stroke with a mismatch between deficit and infarct. *N Engl J Med* 2018;378:11–21.
- Kelly AG, Holloway RG. Guideline: the AHA/ASA made 217 recommendations for early management of acute ischemic stroke in adults. *Ann Intern Med* 2018;168:JC63.
- Albers GW, Lansberg MG, Kemp S, *et al.* A multicenter randomized controlled trial of endovascular therapy following imaging evaluation for ischemic stroke (defuse 3). *Int J Stroke* 2017;12:896–905.
- Chamorro Á, Dirnagl U, Urra X, *et al.* Neuroprotection in acute stroke: targeting excitotoxicity, oxidative and nitrosative stress, and inflammation. *Lancet Neurol* 2016;15:869–81.
- Zang J, Lu D, Xu A. The interaction of CircRNAs and RNA binding proteins: an important part of circRNA maintenance and function. *J Neurosci Res* 2020;98:87–97.

- 28 Lu D, Ho ES, Mai H, *et al.* Identification of blood circular RNAs as potential biomarkers for acute ischemic stroke. *Front Neurosci* 2020;14:81.
- 29 Lu D, Xu AD. Mini review: circular RNAs as potential clinical biomarkers for disorders in the central nervous system. *Front Genet* 2016;7:53.
- 30 Qu L, Yi Z, Shen Y, *et al.* Circular RNA vaccines against SARS-Cov-2 and emerging variants. *Cell* 2022;185:1728–44.
- 31 Zhang C, Zhang B. RNA therapeutics: updates and future potential. *Sci China Life Sci* 2023;66:12–30.
- 32 Hong CA, Nam YS. Functional nanostructures for effective delivery of small interfering RNA therapeutics. *Theranostics* 2014;4:1211–32.
- 33 Wang C, Lin G, Luan Y, *et al.* HIF-Prolyl hydroxylase 2 silencing using siRNA delivered by MRI-visible nanoparticles improves therapy efficacy of transplanted Epcs for ischemic stroke. *Biomaterials* 2019;197:229–43.
- 34 Lin B, Lu L, Wang Y, *et al.* Nanomedicine directs neuronal differentiation of neural stem cells via silencing long noncoding RNA for stroke therapy. *Nano Lett* 2021;21:806–15.
- 35 Piperno A, Sciortino MT, Giusto E, *et al.* Recent advances and challenges in gene delivery mediated by polyester-based nanoparticles. *Int J Nanomedicine* 2021;16:5981–6002.
- 36 Rai R, Alwani S, Badea I. Polymeric nanoparticles in gene therapy: new avenues of design and optimization for delivery applications. *Polymers (Basel)* 2019;11:745.
- 37 Arima H. Twenty years of research on cyclodextrin conjugates with PAMAM dendrimers. *Pharmaceutics* 2021;13:697.
- 38 Chen J, Jin J, Li K, *et al.* Progresses and prospects of neuroprotective agents-loaded nanoparticles and biomimetic material in ischemic stroke. *Front Cell Neurosci* 2022;16:868323.
- 39 Yuan J, Li L, Yang Q, *et al.* Targeted treatment of ischemic stroke by bioactive nanoparticle-derived reactive oxygen species responsive and inflammation-resolving nanotherapies. *ACS Nano* 2021;15:16076–94.

1 **Supplementary file**

2 **Penumbra-Targeted CircOGDH siRNA-Loaded Nanoparticles Alleviate Neuronal Apoptosis**

3 **in Focal Brain Ischemia**

4

5 **Materials and methods**

6 **Materials**

7 PLGA-COOH (LA: GA = 50: 50, Mn =13000) was assembled, Polyamide amine (PAMAM)
8 generation five and Tween 80 were purchased from Sigma-Aldrich (St. Louis, MO, USA).
9 CY5.5-NHS was purchased from RuixiBio (Xi-an, China, catalog #: R-FR-005). The water used
10 in all experiments was distilled water (DW). The primer sequences of CircOGDH and β -actin
11 were as followed: CircOGDH Forward: AACTCGTGGAGGACCACTTG, Reverse:
12 GAGCTTCGACTCAGGGAAAG, β -actin Forward: ACGGCCAGGTCATCACTATTG, Reverse:
13 CAAGAAGGAAGGCTGGAAAAGA.

14

15 **Assembly of PLGA-PAMAM@ CircOGDH siRNA nanoparticles**

16 PLGA-PAMAM was assembled as following: 21mg of PLGA-COOH were dissolved in 3 mL of
17 acetone, the mixed solution then was stirred at room temperature until PLGA-COOH completely
18 dissolved. 45mg of Tween 80 were dissolved in 5 mL of DW, then the dissolved PLGA-COOH
19 mixed solution was added dropwise under stirring overnight at room temperature. PAMAM
20 solution (generation 5, Sigma-Aldrich, St. Louis, USA, catalog #:163442-68-0) was added to the
21 PLGA-COOH reaction mixed solution under stirring for 12 hours at room temperature. The final
22 product PLGA-PAMAM nanoparticles were isolated by ultrafiltration using 100k MWCO
23 centrifugal filter (Millipore, USA, catalog #: UFC901096).

24

25 CircOGDH siRNA or CY3 labeled CircOGDH siRNA (Gene Pharma, Shanghai, China) was
26 dissolved in 500 μ L of DW, then CircOGDH siRNA solution was added dropwise into PLGA-
27 PAMAM mixed solution under stirring overnight at 4°C. The sequences of CircOGDH siRNA
28 were as followed: 5' to 3' CACAGACAAACUUGUCAUGTT.

29

30 **Characterization of PLGA-PAMAM@ CircOGDH siRNA nanoparticles**

31 The zeta potential, size distribution and morphology of PLGA-PAMAM, PLGA-PAMAM@
32 CircOGDH siRNA were characterized by Zetasizer Nano ZS particle analyzer (Malvern, England)
33 and transmission electron microscope (TEM, Hitachi H-7650, 100 kV). TEM samples were
34 prepared by dispersing nanoparticles on copper grids. Elemental mapping of PLGA-PAMAM@
35 CircOGDH siRNA nanoparticles were obtained using high-resolution transmission electron
36 microscopy (HR-TEM, JEM 2100F). The spectroscopic analysis of PLGA-PAMAM@
37 cy3-CircOGDH siRNA nanoparticles used UV spectrophotometry (UH 4150 Spectrophotometer,
38 Hitachi).

39

40 **Determination of siRNA complexation by gel electrophoresis assay**

41 The encapsulation degree between CircOGDH siRNA and PLGA-PAMAM nanoparticles was
42 evaluated by agarose gel electrophoresis assays using 1.5% agarose gel electrophoresis at 120 V
43 for 20 min. Images was obtained using an ImageQuant LAS 500 Gel analyzer (USA).

44 Quick-Load® 1000 bp DNA Ladder (New England BioLabs, USA, catalog #: NO467S) was used
45 as a DNA marker.

46

47 **Animals**

48 A total of 176 adult male BALB/c mice (22.0-25.5 g, 5 to 7 weeks) were purchased from the
49 Institute of Laboratory Animal Science of the Chinese Academy of Medical Sciences (Guangzhou,
50 China). Mice were housed in a strict constant temperature and humidity. Food and water were
51 available all day and night. The study was carried out in accordance with the recommendations of
52 the NIH Guide (NIH Publications No. 8023, revised 1978) for the Care and Use of Laboratory
53 Animals. All experiments were carefully conducted in accordance with the guidelines for Animal
54 Experimentation of Jinan University. The protocol was approved by the Ethics Committee of the
55 Institute of Laboratory Animal Science of Jinan University.

56

57 **Middle cerebral artery occlusion reperfusion (MCAO/R) and cerebral blood flow (CBF)** 58 **measurement**

59 Adult BALB/c mice were anesthetized with isoflurane (4% for initiating anesthesia in a chamber
60 and 1.5% for maintaining anesthesia afterward; RWD Life Science, Shenzhen, China, catalog #:
61 R510-22-16). A midline incision was made at the neck region and the left carotid artery, external
62 carotid artery and internal carotid artery were isolated. The focal ischemia was induced as our
63 described previously¹ using a filament made of nylon string coated with silicon
64 (MSMC23B104PK100, RWD Life Science, Shenzhen, China) which was inserted into the middle
65 cerebral artery (MCA) for 40 minutes, then the silicone tip was removed for reperfusion. Cerebral
66 blood flow was monitored using a Laser Speckle Contrast Imaging (PeriCam PSI System, Perimed
67 AB, Stockholm, Sweden) according to the manufacturer's instructions to confirm successful
68 MCAO and MCAO/R. Mice were immediately put into a 37 °C chamber for 15 minutes and then
69 back to a normal cages.

70

71 ***In vivo* cellular uptake of PLGA–PAMAM@ CircOGDH siRNA nanoparticles**

72 Three days after tail intravenously injection of CY3 labeled PLGA–PAMAM@ CircOGDH
73 siRNA nanoparticles in MCAO-reperfusion mice, mice were fixed by heart perfusion with cool
74 physiological saline solution, followed by 30 ml of 4% paraformaldehyde (Biosharp, Hefei, China,
75 catalog #BL539A). Then brains were collected for preparing tissue sections. Before being
76 embedded with in optimal cutting temperature (OCT) compound, brain tissues were orderly
77 immersed in 20%, 30% sucrose-distilled water overnight at 4 °C. Finally, brain sections were cut
78 into 10 µm slices using a cryostat (Thermo Fisher Scientific, Waltham, MA, USA). The brain
79 sections were incubated with the following primary antibody: Fluorescent Nissl staining (1:200;
80 Thermo Fisher Scientific, Waltham, MA, USA, catalog #: N21483), anti-glial fibrillary acidic
81 protein antibody (anti-GFAP; 1:100; Cell Signaling Technology, Danvers, MA, USA, catalog #:
82 3670S), anti-ionized calcium-binding adaptor molecule 1 antibody (Iba-1; 1:100; Abcam, catalog
83 #: ab5076) overnight at 4 °C, followed by incubation with a mixture of fluorescent secondary
84 antibodies for 1 h at room temperature. Then brain sections were stained with
85 3,3-diaminobenzidin for 5 minutes at room temperature. Images were captured using a confocal
86 microscope (Carl Zeiss LSM700, Vizna, Germany).

87

88 In Vivo fluorescence imaging of PLGA–PAMAM in MCAO/R Mice

89 CY5.5-NHS (Ruixi, Xian, China, catalog #R-FR-005) labeled PLGA–PAMAM nanoparticles
90 were assembled as following: CY5.5-NHS was dissolved in DMSO, 8µL of 10 mg/mL
91 CY5.5-NHS solution was added to a total of 1mL PLGA–PAMAM solution. Finally, it was stirred
92 for 12h at room temperature. The CY5.5-labeled PLGA–PAMAM nanoparticles were collected by
93 centrifugation. 100 µL CY5.5-labeled PLGA–PAMAM nanoparticles were tail intravenously
94 injected into MCAO/R mice. Fluorescence was monitored using the In Vivo animal imaging
95 system (NightOWL II LB 983) at 0.5, 1.5, 2.5 h and day 3.

96

97 Mice behavioral tests

98 Mice were coded and were randomly divided into three groups: SHAM, MCAO/R + PLGA–
99 PAMAM, MCAO/R + PLGA–PAMAM@ CircOGDH siRNA. Mice behavioral tests were
100 performed by an independent investigator who was blind to the experimental groups and the data
101 was analyzed by separate investigator.

102

103 For the grid-walking task, an elevated grid area of 32 cm × 20 cm × 50 cm (length × width ×
104 height) made of 12 mm square wire mesh was used. Mice were placed individually on the wire
105 grid and allowed to freely move for 3 minutes. A camera was positioned beneath the grid to record
106 stepping errors (foot faults). The numbers of foot faults and non-faults for each limb were counted.
107 A ratio was calculated as follows: number of foot faults / (number of foot faults + number of
108 non-faults) × 100%.

109

110 For the cylinder test, mice were placed inside a plastic cylinder (15 cm tall with a diameter of 10
111 cm) and videotaped for 5 minutes. The score was calculated as the ratio: (number of left hand –
112 number of right hand) / (number of right hand + number of left hand + number of both hands).

113

114 For the adhesive removal somatosensory test, 2 small pieces of adhesive-backed paper dots of
115 equal size (25 mm²) were used as bilateral tactile stimuli occupying the distal-radial region on the
116 wrist of each forelimb. The time for mice to remove each stimulus from the forelimb was recorded
117 and the time exceeded 120 s were recorded as 120 s. Before surgery, animals were trained for 3
118 days. Once mice were able to remove the dots within 10 s, they were subjected to ischemic stroke.

119

120 MRI for mice

121 MRI for mice was conducted using a 9.4 tesla small animal MRI scanner (Bruker PharmaScan).
122 Mice were anesthetized using 2% isoflurane through a nose cone, and the body temperature and
123 respiratory rate were monitored. T2 MRI imaging was conducted at day3 after MCAO/R using a
124 2D fast-spin echo sequence. (T2 MRI: 2D fast-spin echo sequence (3500/33 ms of repetition
125 time/echo time, 2 average). 17 axial slices with a slice thickness of 0.7 mm, a matrix of 256 ×256,
126 and an FOV of 20 × 20 mm). It was positioned over the brain, excluding the olfactory bulb. Under
127 the same scale and brain slices of MCAO mouse images, T2 MRI imaging was scanned and
128 quantified using RadiAnt DICOM Viewer software (<https://radiantviewer.com/trial>).

129

130 Nissl staining

131 As described above¹, three days after tail intravenously injection of nanoparticles in

132 MCAO-reperfusion mice, mice were fixed by heart perfusion and finally, brain sections were cut
133 into 10 μm slices using a cryostat (Thermo Fisher Scientific, Waltham, MA, USA). Nissl staining
134 experiment was performed using the Nissl staining assay kit (Beyotime Biotechnology, Shanghai,
135 China, catalog # C0117) following the manufacturer's instructions³⁷ or Fluorescent Nissl dye
136 (1:200; Thermo Fisher Scientific, Waltham, MA, USA, catalog # N21483). Brain slices were
137 sealed with neutral gum and images were captured using light microscope (Leica
138 DMILLED/ICC50HD, Solms, Germany). Quantification was performed using image J software
139 (Bethesda, MD, USA). Researchers were blinded to the experimental conditions for data analysis.

140

141 **Tunel staining**

142 As described above¹, three days after tail intravenously injection of nanoparticles in
143 MCAO-reperfusion mice, mice were fixed by heart perfusion and brain sections were cut into 10
144 μm slices using a cryostat (Thermo Fisher Scientific, Waltham, MA, USA). A one-step TUNEL
145 apoptosis assay kit (Beyotime, Beijing, China, CATALOG#: C1089) was used to detect apoptosis
146 according to the manufacturer's instructions. Brain slices were washed in PBS and subsequently
147 incubated with 0.1% Triton X-100 in PBS for 2 min at room temperature. After washed in PBS for
148 three times, brain slices were then incubated in TUNEL solution in the dark for 1 h at room
149 temperature. Finally, sections were stained with Fluorescent Nissl dye (1:200; Thermo Fisher
150 Scientific, Waltham, MA, USA, catalog # N21483) and DAPI (Beyotime, Beijing, China,
151 CATALOG#: C1005). Images were captured using light microscope (Leica DMILLED/ICC50HD,
152 Solms, Germany). Quantification was performed using image J software (Bethesda, MD, USA).

153

154 **RNA extraction and RT-qPCR**

155 Brain tissue was collected into a tube on the ice for RNA extraction using Trizol Reagent
156 according to the manufacturer's instructions. For RT-qPCR, RNA was performed
157 reverse-transcription with corresponding primers for β -actin (Forward:
158 ACGGCCAGGTCATCACTATTG, Reverse: CAAGAAGGAAGGCTGGAAAAGA), CircOGDH
159 (Forward: AACTCGTGGAGGACCACTTG, Reverse: GAGCTTCGACTCAGGGAAAG) (Gene
160 Pharma, Shanghai, China) using the Prime Script RT Master Mix (Takara, Japan, catalog
161 #:RR047A) following the manufacturer's protocol. Real-time PCR was conducted using
162 LightCycler® 480 SYBR Green I Master (Roche, United States, catalog #:04887352001)
163 following the manufacturer's instructions. Thermocycle conditions used in amplification: Pre
164 incubation at 95 °C for 10 min, amplification using 40 cycles of 95 °C for 10 sec, 55-60°C for
165 20sec, and 72 °C for 30 sec, followed by 75 °C to 94 °C with increment of 0.5 for 5 sec, finally at
166 40°C for 10 sec. The comparative CT method referred to as the $2^{-\Delta\Delta\text{CT}}$ method², a widely used
167 method. Relative gene expression in each group were normalized by internal control and then
168 compared with that in corresponding control.

169

170 **Primary neuron culture**

171 Primary cortical neurons were obtained from the cerebral cortex of BALB/c mouse embryos
172 (E18-E19) purchased from the Institute of Laboratory Animal Science of the Chinese Academy of
173 Medical Sciences (Guangzhou, China). As described above¹, the cerebral cortex was isolated and
174 gently pipetted and then the cell suspension was collected in a new centrifuge tube. Cells were
175 digested in 0.125% trypsin for 15 minutes at 37 °C and after filtered with a 70 μm cell strainers

176 (Corning, New York, USA, catalog #:352350). Filtrates were collected and then centrifuged at
177 1000 rpm for 5 minutes. Cells were resuspended in DMEM/F-12 containing 10% FBS (Gibco,
178 United States, catalog #: C11330500) and 1% penicillin-streptomycin (Biological Industries,
179 Kibbutz Beit-Haemek, Israel, catalog #: 03-031-1B), and then seeded on 6-well plates pre-coated
180 with poly-L-lysine (Sigma-Aldrich, St. Louis, USA, catalog #: P1274). Cells were cultured for 4
181 hours in a humidified incubator (37 °C, 5% CO₂), and then medium was changed with complete
182 medium which contained neurobasal medium (Gibco, Waltham, MA, USA) supplemented with
183 B-27™ Supplement (Gibco, Waltham, MA, USA, catalog #: 17504-044) and 1%
184 penicillin-streptomycin liquid. Medium was changed by half every three days. Neurons cultured
185 after day 5 were used for experiments.

186 For ischemic treatments, neurons were mainly divided into two groups: (1) control (CON):
187 neurons were incubated in neuronal complete medium in a regular humidified incubator (37°C, 5%
188 CO₂). (2) OGD/R: neurons were exposed to DMEM solution without glucose in an incubator
189 containing 0 % O₂, 5 % CO₂ with balanced N₂ for 3 hours, followed by reperfusion for 24 hours.
190 SH-SY5Y cells were obtained from American Type Culture Collection and cultured in DMEM
191 containing 10% FBS in a humidified incubator (37 °C, 5% CO₂).

192

193 ***In vitro* neuron uptake of PLGA–PAMAM@ CircOGDH siRNA nanoparticles**

194 Cy3 labeled PLGA–PAMAM@ CircOGDH siRNA nanoparticles were added into primary cortical
195 neurons at day 5 for 24h, primary cortical neurons were cultured in confocal petri dishes, rinsed
196 with PBS and fixed with 4% PFA for 15 min at room temperature. Cells were then washed in PBS
197 twice and permeabilized with PBS containing 0.3% Triton X-100 for 20 min and blocked with 5%
198 bovine serum albumin (BSA) for 60 min at room temperature. Cells were stained with fluorescent
199 Nissl dye (1:200; Thermo Fisher Scientific, Waltham, MA, USA, catalog #: N21480) for 20
200 minutes at room temperature, followed by 3,3-diaminobenzidin for 5 minutes. After PBS washing
201 for three times, cells were mounted and images were captured using a confocal microscope (Carl
202 Zeiss LSM700, Vizna, Germany).

203

204 **CCK8 assay**

205 Cell viability was assessed by the Cell Counting Kit 8 (CCK8, Beyotime Biotechnology, Shanghai,
206 China, catalog #: C0039) according to manufacturer's instruction. Neurons were seeded at 2×10^4
207 cells per well on 96-well plates and the OD450 was measured using a microplate reader (Thermo
208 Fisher Scientific, Waltham, MA, USA). Data were normalized and calculated by the
209 corresponding control group.

210

211 **Cellular fluorescence localization of PLGA–PAMAM@ CircOGDH siRNA nanoparticles**

212 Intracellular localization of cy3 labeled PLGA–PAMAM@ CircOGDH siRNA was detected by
213 fluorescence microscopy. Primary cortical neurons were cultured in confocal petri dishes for 5-6
214 days, and then incubated with 2.5µL 100 µg/mL of cy3 labeled PLGA–PAMAM@ CircOGDH
215 siRNA for various times including 3h, 6h, 9h, 12h and 24h. Cells were rinsed with PBS twice and
216 incubated with lysotracker (Life technologies, Waltham, MA, USA, catalog #L12492) for 1h in a
217 humidified incubator (37 °C, 5% CO₂), then fixed with 4% PFA for 15 min at room temperature.
218 Cells were stained with fluorescent Nissl dye (1:200; Thermo Fisher Scientific, Waltham, MA,
219 USA, catalog #: N21480) for 20 minutes at room temperature, followed by 3,3-diaminobenzidin

220 for 5 minutes. After PBS washing for three times, cells were mounted and images were captured
221 using a confocal microscope (Carl Zeiss LSM700, Vitzna, Germany).

222

223 **Flow cytometry in SH-SY5Y cells**

224 SH-SY5Y cells were seeded at 18×10^4 cells per well on 6-well plate and PLGA–
225 PAMAM@cy3-CircOGDH siRNA, cy3-CircOGDH siRNA were added for 48 hours. After
226 washed with cold PBS three times, SH-SY5Y cells were collected in 300 ul of PBS and used for
227 flow cytometry (Canto, BD, USA).

228

229 **Western blot analysis**

230 Protein extracts obtained from neurons were subjected to SDS polyacrylamide gels (12%)
231 electrophoresis and electrically transferred to a polyvinylidene difluoride membrane before
232 incubated with specific antibodies. Primary antibodies against the following proteins were used:
233 COL4A4 (1:1000; Proteintech), BCL-2 (catalog #: 15071S), β -actin (catalog #: 4970S), BAX
234 (catalog #: 5023S), cleaved caspase 3 (catalog #: 9664S) (1:1000; Cell Signaling Technology).
235 After incubation with primary antibodies overnight at 4 °C, membranes were incubated for 1 hour
236 with the appropriate secondary antibody (anti- Rabbit IgG H&L (HRP), catalog #: ab97051). The
237 antibodies were visualized by enhanced chemiluminescence (ECL Plus; Wanleibio, Shenyang,
238 China, catalog #: WLA006c). Image J software was used to quantify the band intensity, each value
239 was normalized by β -actin. Then the ratio of COL4A4, BCL2/BAX and cleaved caspase3 in each
240 group were compared with that in control group.

241

242 **Toxicity tests of PLGA–PAMAM@ CircOGDH siRNA nanoparticles *in Vivo***

243 The MCAO-reperfusion mice were treated with 100 μ L 100 μ g/mL PLGA–PAMAM@ CircOGDH
244 siRNA nanoparticles. After treatment for 3 days, whole blood was collected and centrifuged to
245 obtain serum for detection of RBC, WBC, PLT numbers. Hematology analysis was used to
246 evaluate the toxicity of PLGA–PAMAM and PLGA–PAMAM@ CircOGDH siRNA nanoparticles
247 *in vivo*, including effects on alanine aminotransferase (ALT), aspartate transaminase (AST) and
248 creatinine (CREA), correspondingly, liver and kidney tissues were collected for H&E staining and
249 pathological analysis.

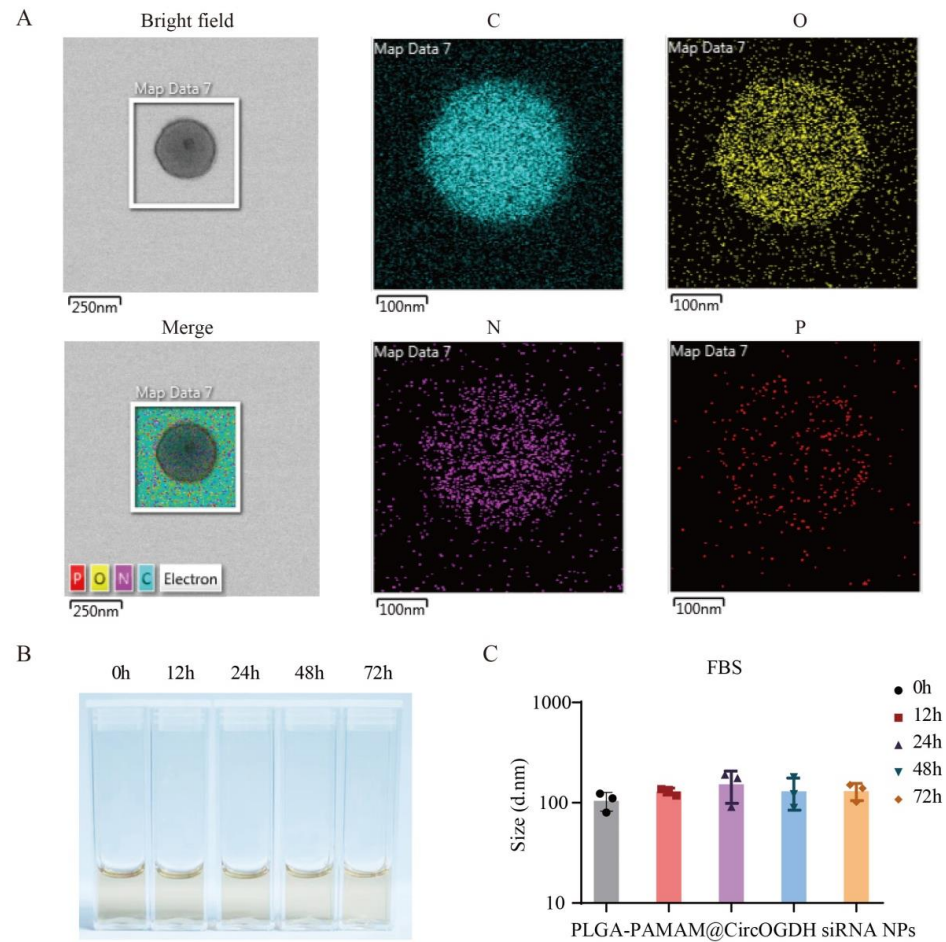
250

251 **Statistics**

252 All statistical analyses were performed using SPSS (Windows version 27.0; SPSS Inc., Chicago,
253 IL, USA) or GraphPad Prism 8.01 software (GraphPad Software, Inc., La Jolla, CA, USA). Data
254 were expressed as mean \pm SD. For experiments with small sample size ($n < 6$), power calculations
255 were not performed and p-values were determined by non-parametric analysis (Mann-Whitney
256 test). Otherwise, Shapiro-Wilk test was used for normality test with a threshold of 0.05, for data
257 with normal distribution, Student's t-tests (two-tailed) or one-way ANOVA were determined, and
258 for data without normal distribution, Mann-Whitney test was used. P-values of 0.05 or less were
259 considered statistically significant. All representative images were selected without bias, and had
260 characteristics typical of the data or overall trend.

261 **Supplementary Figure**

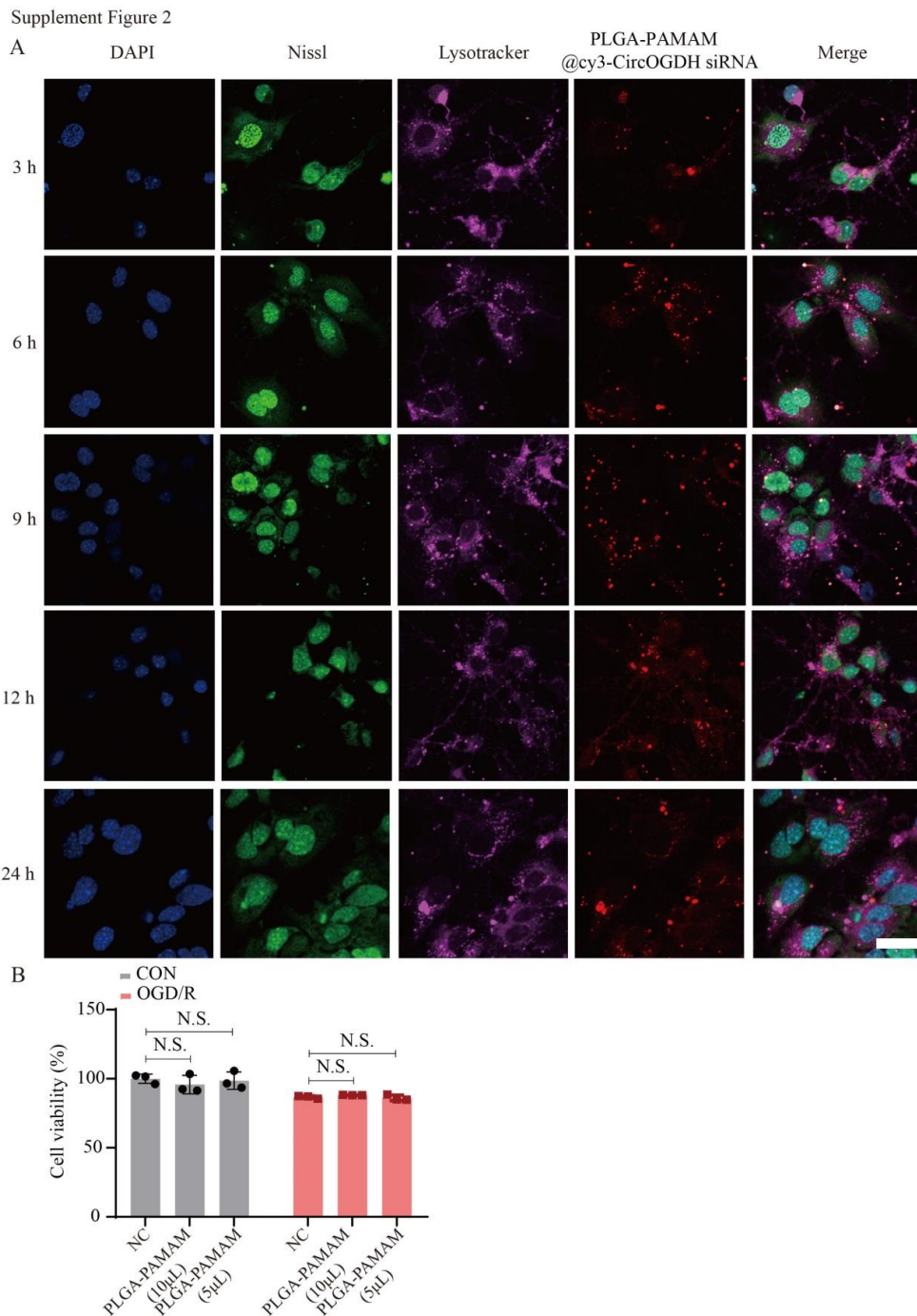
Supplement Figure 1



262

263 **Supplementary Figure 1. Characterization of PLGA-PAMAM@CircOGDH siRNA**264 **nanoparticles. (A).** Elemental mapping of PLGA-PAMAM@CircOGDH siRNA nanoparticles.265 Scale bar = 100 nm. **(B-C).** Stability of PLGA-PAMAM@CircOGDH siRNA nanoparticles in266 FBS solution at different time points. Data are presented as means \pm SD; n = 3.

267



268

269

270

271

272

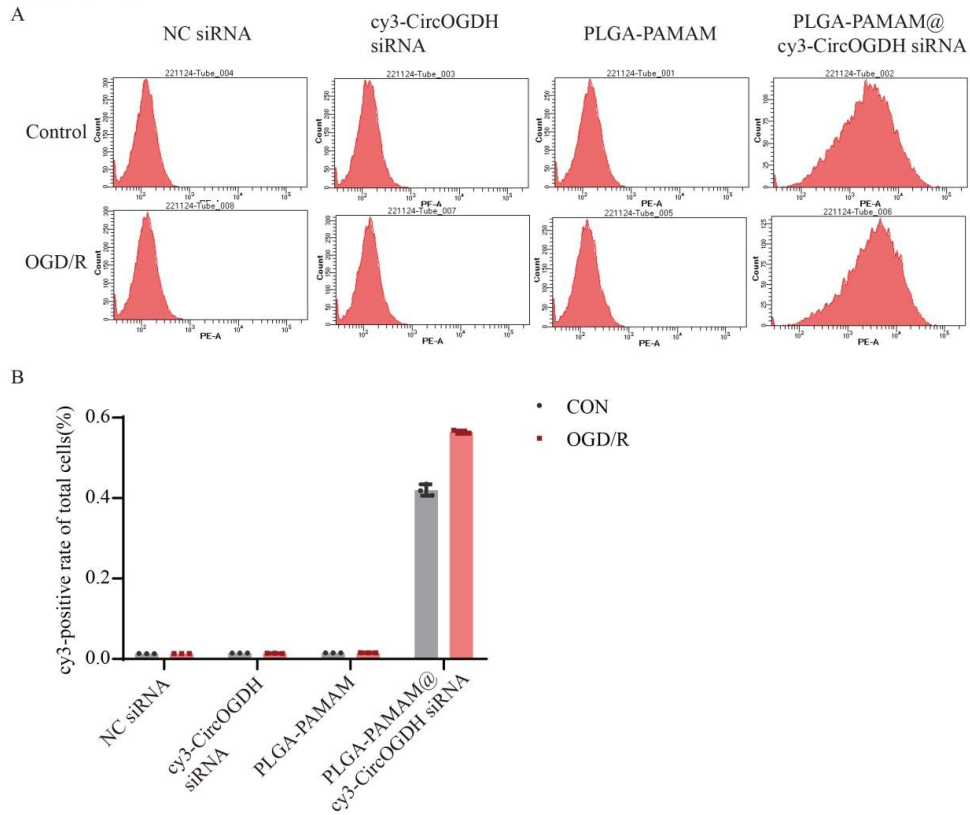
273

274

Supplementary Figure 2. Cellular uptake of PLGA–PAMAM@CircOGDH siRNA nanoparticles in primary cortical neurons. **(A)** Intracellular trafficking of PLGA–PAMAM@Cy3-CircOGDH siRNA nanoparticles (red) in primary neurons at 3 h, 6 h, 9 h, 12 h, and 24 h. Neurons were stained with Nissl (green). Lysotracker staining is shown in cherry. Nuclei were stained with DAPI (blue). Scale bar = 50 µm. **(B)** Cell viability was determined in primary cortical neurons treated with normal control (NC) and PLGA–PAMAM nanoparticles. Data were presented as mean± SD;

275 n=3, Mann–Whitney U test.
276

Supplement Figure 3



277

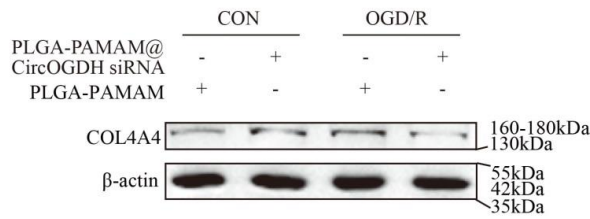
278 **Supplementary Figure 3. Cellular uptake of PLGA-PAMAM@CircOGDH siRNA**279 **nanoparticles in SH-SY5Y cells. (A-B).** Detection of the cy3-positive cells percentage in four

280 groups by flow cytometry analysis. Data were presented as mean± SD; n=3.

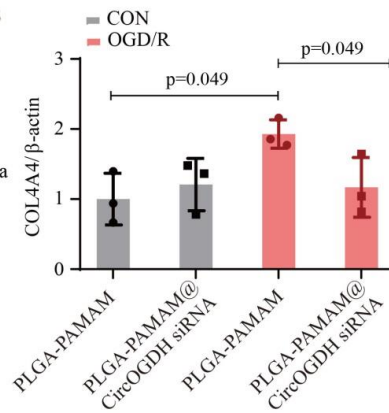
281

Supplement Figure 4

A



B

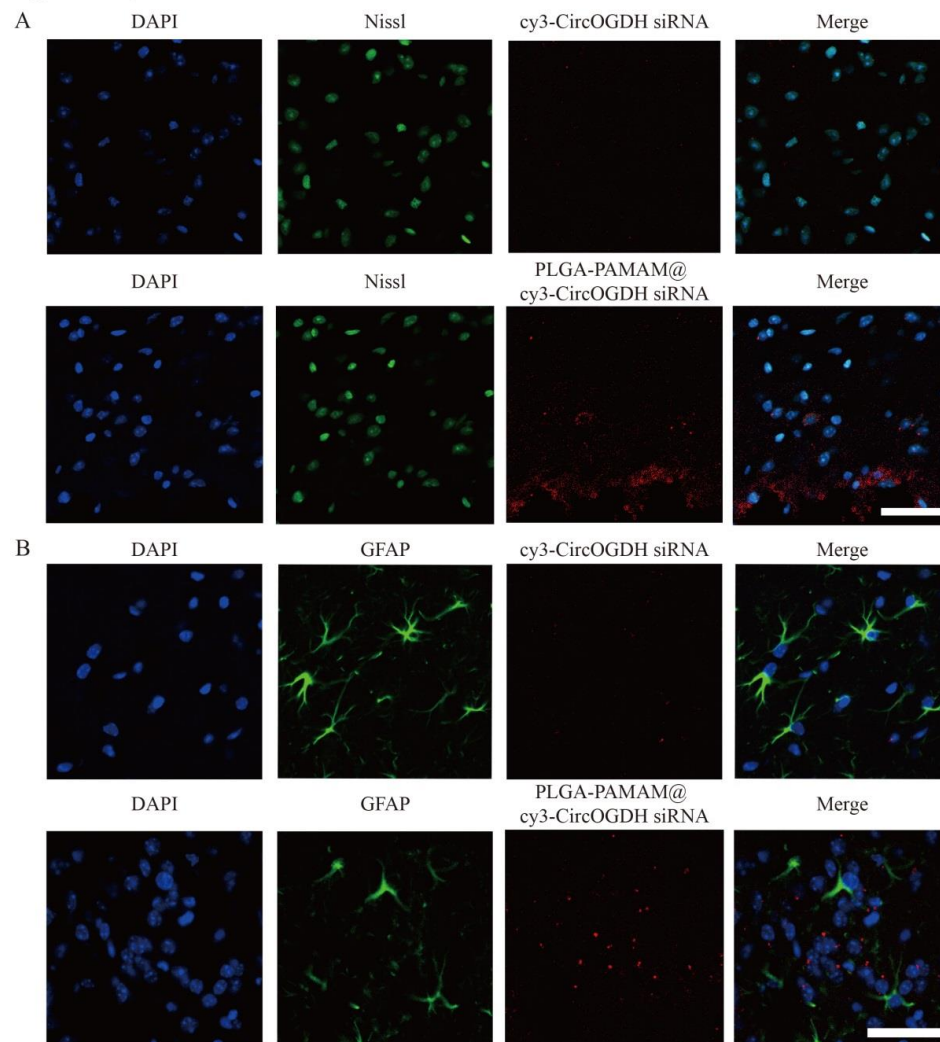


282

283 **Supplementary Figure 4. PLGA-PAMAM@CircOGDH siRNA nanoparticles downregulated**
 284 **COL4A4 protein expression level. (A-B).** Western blot analysis of COL4A4 expression level in
 285 control (CON) and ischemic-reperfusion (OGD/R) neurons treated with PLGA-PAMAM and
 286 PLGA-PAMAM@CircOGDH siRNA nanoparticles. Data were presented as mean± SD; n=3,
 287 Mann-Whitney U test.

288

Supplement Figure 5



289

290 **Supplementary Figure 5. Uptake of PLGA–PAMAM@CircOGDH siRNA nanoparticles in**291 **penumbra tissue cells of mice brain. (A).** Immunofluorescence experiments showed the

292 localization of PLGA–PAMAM@cy3-CircOGDH siRNA nanoparticles (red) with Nissl staining

293 (green) in the penumbra tissue of mice brain. Nuclei were stained with DAPI. Scale bar, 50 μm.

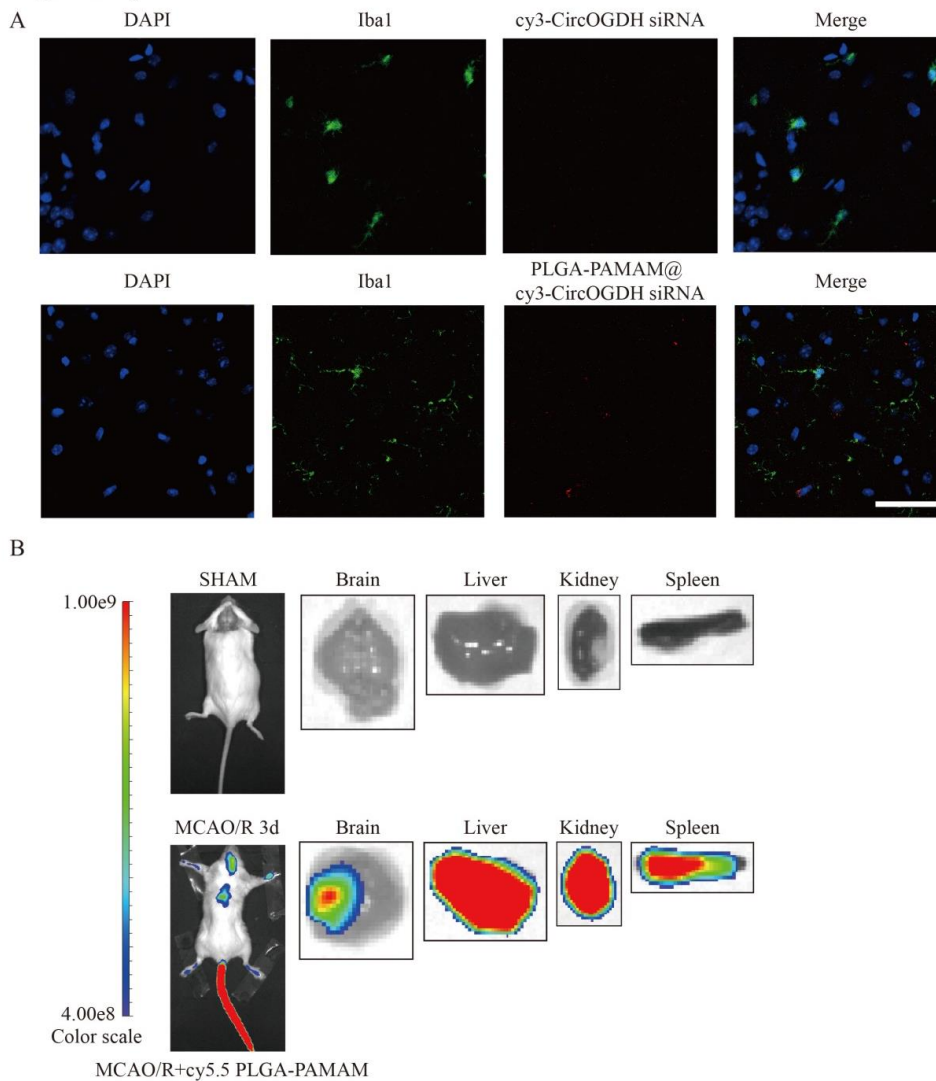
294 **(B).** Immunofluorescence experiments showed the localization of PLGA–

295 PAMAM@cy3-CircOGDH siRNA nanoparticles (red) with GFAP staining (green) in the

296 penumbra tissue of mice brain. Nuclei were stained with DAPI. Scale bar, 50 μm.

297

Supplement Figure 6



298

299

300

301

302

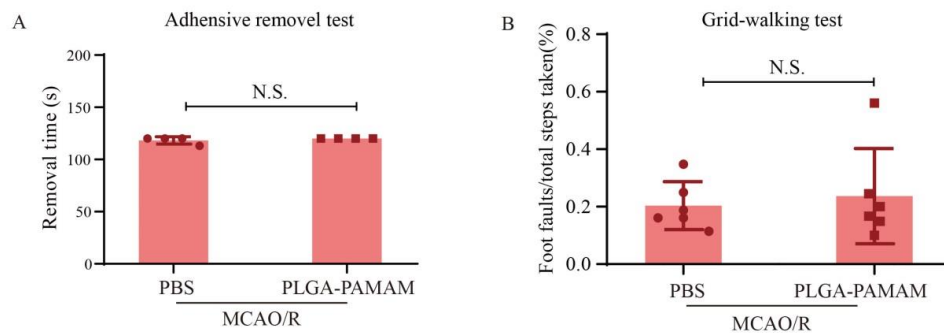
303

304

305

Supplementary Figure 6. Uptake of PLGA–PAMAM@CircOGDH siRNA nanoparticles in mice. (A). Immunofluorescence experiments showed the localization of PLGA–PAMAM@cy3–CircOGDH siRNA nanoparticles (red) with Iba1 staining (green) in the penumbra tissue of mice brain. Nuclei were stained with DAPI. Scale bar, 50 μ m. (B). *In vivo* fluorescence imaging of Cy5.5-labelled PLGA–PAMAM nanoparticles in MCAO/R mice at day 3. Units of the color scale: perfusion units (PUs).

Supplement Figure 7



306

307 **Supplementary Figure 7. PLGA-PAMAM nanoparticles showed no effect in MCAO/R mice.**

308 (A-B). PLGA-PAMAM nanoparticles showed no effect in MCAO/R mice 3 days after tail

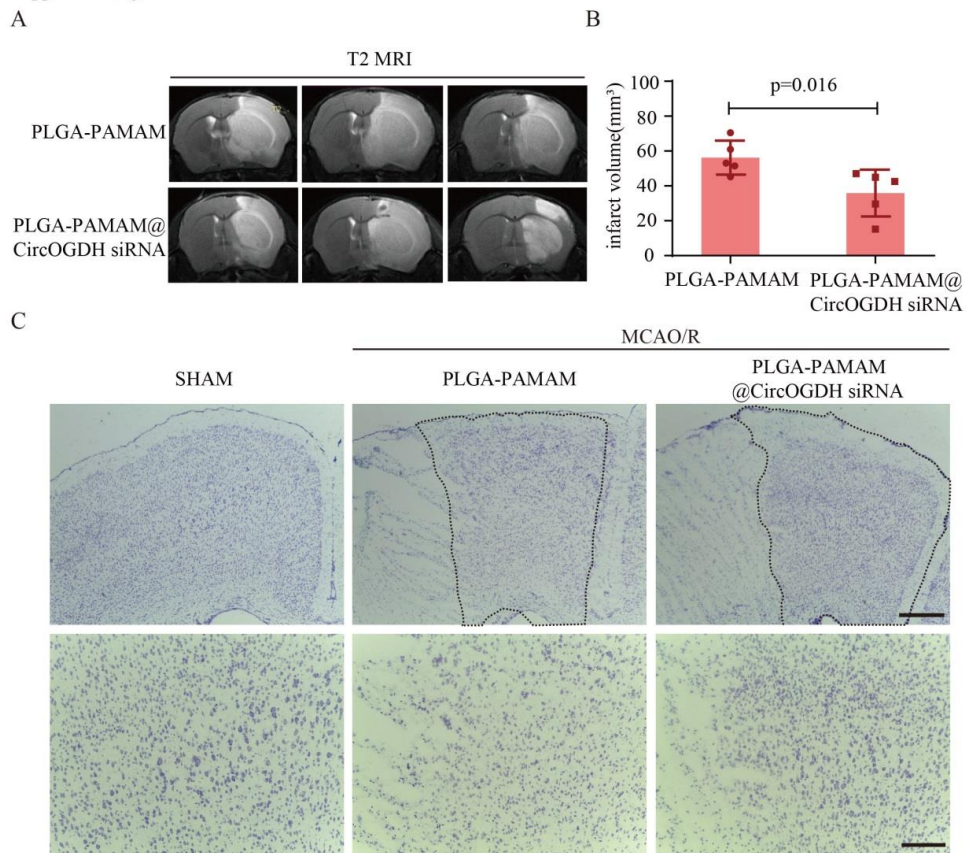
309 injection, as demonstrated by the adhesive removal test (A), grid-walking test (B). Data are

310 presented as means \pm SD. Adhesive removal test: n = 3-4 in each group; grid-walking test: n = 4 in

311 the SHAM group, n = 6 in the MCAO/R+PLGA-PAMAM group, Mann-Whitney U test.

312

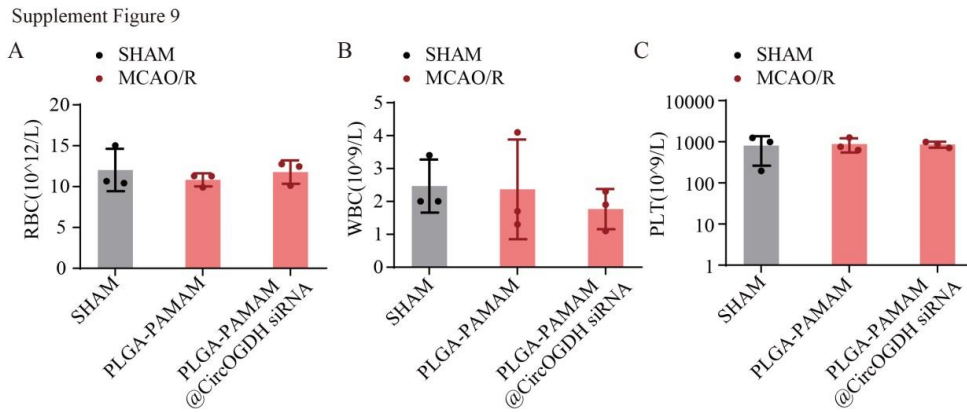
Supplement Figure 8



313

314 **Supplementary Figure 8. (A–B)** Representative images showing T2 MRI in MCAO/R mice after
 315 microinjected with PLGA–PAMAM and PLGA–PAMAM@ CircOGDH siRNA nanoparticles for
 316 three days. Data were presented as mean±SD; n=5 for each group, Mann–Whitney U test. **(C)**
 317 PLGA–PAMAM@CircOGDH siRNA increased intact neuron number in MCAO/R mice. Nissl
 318 staining showing the number of neurons in the SHAM, MCAO+PLGA–PAMAM, and
 319 MCAO+PLGA–PAMAM@CircOGDH siRNA groups 3 days after tail injection. Scale bar = 500
 320 μm (upper); scale bar = 200 μm (lower).

321



322

323 **Supplementary Figure 9.** PLGA–PAMAM@CircOGDH siRNA increased intact neuron number
324 in MCAO/R mice. (A–C). Hematological analyses of RBC numbers (A), WBC numbers (B), and
325 PLT numbers (C) were performed in the SHAM, MCAO+PLGA–PAMAM, and MCAO+PLGA–
326 PAMAM@CircOGDH siRNA groups 3 days after tail injection. Data were presented as mean±
327 SD; n=3, Mann–Whitney U test.

328

329

330 **References**

- 331 1. Liu Y, Li Y, Zang J, Zhang T, Li Y, Tan Z, Ma D, Zhang T, Wang S, Zhang Y, Huang L,
332 Wu Y, Su X, Weng Z, Deng D, Kwan Tsang C, Xu A, Lu D. Circogdh is a penumbra
333 biomarker and therapeutic target in acute ischemic stroke. *Circulation research*.
334 2022:CIRCRESAHA121319412
- 335 2. Schmittgen TD, Livak KJ. Analyzing real-time pcr data by the comparative c-t method.
336 *Nat Protoc*. 2008;3:1101-1108
- 337

Graphical Abstract

